ARMY RESEARCH LABORATORY

Results of Bare Die Testing of Optimized (2nd Pass) Gallium Arsenide (GaAs) Integrated Circuit Radio Frequency (RF) Booster Designs for 425 MHz and Dual Band (425 and 900 MHz)

by John E. Penn

ARL-TR-5465 **February 2011**

NOTICES

Disclaimers

The findings in this report are not to be construed as an official Department of the Army position unless so designated by other authorized documents.

Citation of manufacturer's or trade names does not constitute an official endorsement or approval of the use thereof.

Destroy this report when it is no longer needed. Do not return it to the originator.

Army Research Laboratory
Adelphi, MD 20783-1197

ARL-TR-5465 **February 2011**

Results of Bare Die Testing of Optimized (2nd Pass) Gallium Arsenide (GaAs) Integrated Circuit Radio Frequency (RF) Booster Designs for 425 MHz and Dual Band (425 and 900 MHz)

John E. Penn
Sensors and Electron Devices Directorate, ARL

REPORT DOCUMENTATION PAGE

Form Approved
OMB No. 0704-0188

1. REPORT DATE *(DD-MM-YYYY)*	2. REPORT TYPE	3. DATES COVERED (From - To)
February 2011		

4. TITLE AND SUBTITLE
Results of Bare Die Testing of Optimized (2nd Pass) Gallium Arsenide (GaAs) Integrated Circuit Radio Frequency (RF) Booster Designs for 425 MHz and Dual Band (425 and 900 MHz)

5a. CONTRACT NUMBER

5b. GRANT NUMBER

5c. PROGRAM ELEMENT NUMBER

6. AUTHOR(S)
John E. Penn

5d. PROJECT NUMBER

5e. TASK NUMBER

5f. WORK UNIT NUMBER

7. PERFORMING ORGANIZATION NAME(S) AND ADDRESS(ES)
U.S. Army Research Laboratory
ATTN: RDRL-SER-E
2800 Powder Mill Road
Adelphi, MD 20783-1197

8. PERFORMING ORGANIZATION REPORT NUMBER
ARL-TR-5465

9. SPONSORING/MONITORING AGENCY NAME(S) AND ADDRESS(ES)

10. SPONSOR/MONITOR'S ACRONYM(S)

11. SPONSOR/MONITOR'S REPORT NUMBER(S)

12. DISTRIBUTION/AVAILABILITY STATEMENT
Approved for public release; distribution unlimited.

13. SUPPLEMENTARY NOTES

14. ABSTRACT
High-performance microwave and radio frequency integrated circuits (RFICs) are of interest to the Army. Several monolithic microwave integrated circuits (MMICs) were designed to enhance the performance of commercial-off-the-shelf (COTS) RFICs used in many wireless systems. This report documents the bare die probe testing of ten MMIC designs optimized for 400–950 MHz operation. These designs include active RF front end designs, as well as integrated passive matching circuits to reduce SWAP at the system level. Small signal and performance measurements were competed for the designs. A follow-on report will include similar measurements of the active MMICs in packages attached to PC boards for testing.

15. SUBJECT TERMS
MMIC, RFIC, IC

16. SECURITY CLASSIFICATION OF:			17. LIMITATION OF ABSTRACT	18. NUMBER OF PAGES	19a. NAME OF RESPONSIBLE PERSON
a. REPORT	b. ABSTRACT	c. THIS PAGE	UU	62	John E. Penn
Unclassified	Unclassified	Unclassified			19b. TELEPHONE NUMBER (*Include area code*) (301) 394-0423

Standard Form 298 (Rev. 8/98)
Prescribed by ANSI Std. Z39.18

Contents

List of Figures

List of Tables

INTENTIONALLY LEFT BLANK.

1. Introduction

Increased transmission range in low-power radio frequency (RF) applications is desirous for the U.S. Army. The RF integrated circuit (RFIC) booster chip is intended to increase range between RF nodes for low-power wireless applications. The booster concept uses the high RF performance advantages of the gallium arsenide (GaAs) process to enhance the capabilities of systems using commercial RFIC transceivers. It can be inserted easily into systems to increase transmit power, receiver sensitivity, and efficiency or battery usage. In this 2nd pass optimized booster design, lessons learned from a 1st pass design were used to optimize a design for a targeted system performance and battery voltage.

2. Overview of 2nd Pass Designs

The focus of the 2nd pass was predominantly for the 400–450 MHz frequency band, but there was also a desire to have a broadband or dual band capability. Many commercial RFICs are capable over a broad range below 1 GHz but require external matching elements that severely limit the operating band of the system design. In addition to optimizing the RF front end, or Booster integrated circuit (IC), integrated matching circuits were designed to reduce size, weight, and power (SWAP) at the system- or board-level design. As with the 1st pass GaAs IC designs, the 2nd pass tile includes multiple design variations to meet various design goals.

The power amplifiers for the 2nd pass designs were optimized for efficiency at a center frequency of 425 MHz and slightly retuned from the 450 MHz for the 1st pass designs. Also, the power output goals were 50 and 100 mW at 2.8 V, which were to exceed the original 1st pass designs. A secondary goal was operation with similar performance at 3.6 V. The 1st pass power amplifier design was stable and broadband. For the 2nd pass, narrowband amplifiers were designed for good efficiency, good output power, and high gain, primarily for use with a 2.8 V supply voltage. Another goal of the 2nd pass designs was to reduce the insertion loss of the transmit/receive (TR) switch by a factor of two, and to improve overall efficiency and performance of the designs.

There are four active design variations targeting 50 mW at 2.8 V, 100 mW at 2.8 V, and at least 50 mW for either 2.8 V or 3.6 V, plus a dual band design at 425 or 900 MHz using the 1st pass broadband power amplifier design. A broadband BPSK modulator was also created for the dual band design. The fifth active design contains individual probe testable circuits of the narrowband 50-mW power amplifier, the narrowband 100-mW power amplifier, the narrowband 3-mA low noise amplifier, and the broadband TR switch. In addition to the five active IC designs, there are

five passive GaAs IC designs for improving system-level performance by integrating the external RFIC matching circuits into a single IC.

3. Die Testing of Active 2nd Pass Designs

Following is a summary of the active design tests using a probe station for bare die testing. Initial DC biasing of all the circuits was very close to simulations. The TR switch and BPSK modulator circuits draw negligible current. All amplifier designs use a robust current mirror bias, which allows for significant power supply voltage variation with little variation in bias current. Ideally, the battery supplies would be between 2.8 V and 3.6 V, but operation from 2 V to 5 V is possible. Current consumption for the narrowband low noise amplifier was approximately 3 mA, as expected. The broadband low noise amplifier was based on a 1st pass design, but the current mirror was modified to half the power consumption to approximately 8–9 mA. For the dual band design, the broadband power amplifier from the 1st pass was used and consumed approximately 38–40 mA. A new narrowband power amplifier targeted for 50 mW at 2.8 V consumed an expected 38–40 mA. Finally, the high power narrowband power amplifier targeted for 100 mW at 2.8 V consumed 74–78 mA.

- ARL25—This is a test circuit of individual subcircuits from the four active booster IC designs. It contains a 100-mW power amplifier for 2.8 V, a 50-mW power amplifier for 2.8 V, a narrowband low DC power consumption low noise amplifier, and a TR switch.

Simulations for the 50 mW 2.8 V power amplifier from the test circuit were performed in Agilent's ADS simulator and also AWR's Mircrowave Office (MWO) simulator for comparison to probe measurements of the GaAs die. Figure 1 shows the s-parameter comparison of measured data to ADS, and figure 2 shows the same versus MWO. The actual gain is lower than either simulation and the input match is shifted up in frequency. MWO seems to do a much better job of predicting the output match for this circuit.

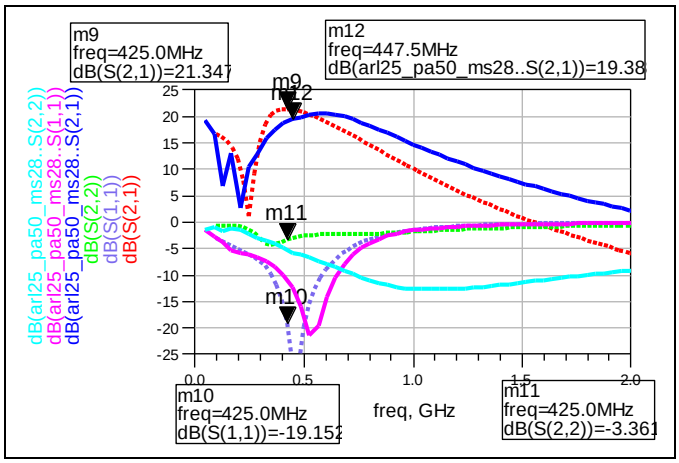

Figure 1. ADS S-parameter simulation (dotted) of 50 mW power amplifier versus measurement (solid).

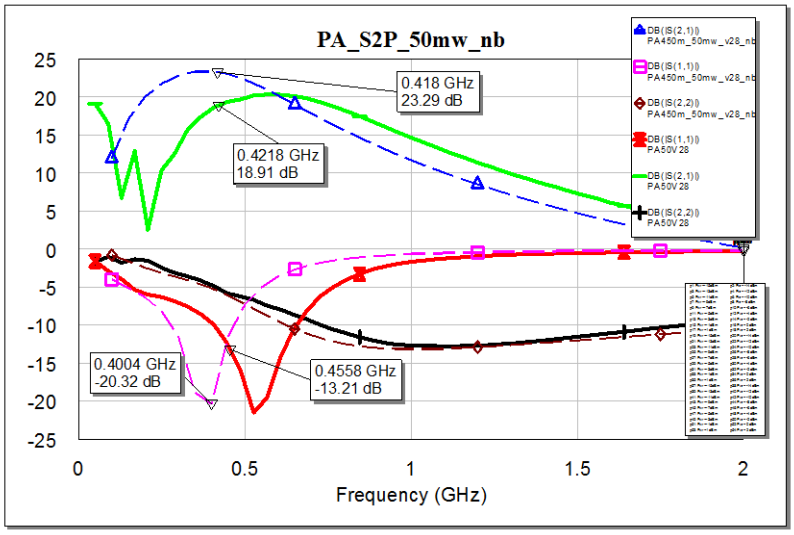

Figure 2. MWO S-parameter simulation (dotted) of 50 mW power amplifier versus measurement (solid).

Simulations for the 100 mW 2.8 V power amplifier from the test circuit were likewise performed with both simulators for comparison to probe measurements of the GaAs die. Figure 3 shows the s-parameter comparison of measured data to ADS, and figure 4 shows the same versus MWO. As in the previous amplifier, the actual gain is lower than either simulation and the input match is shifted up in frequency. MWO seems to do a much better job of predicting the output match for this circuit, as well.

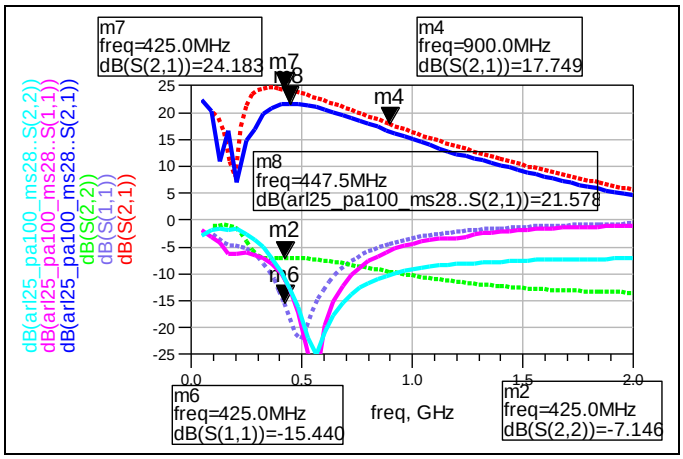

Figure 3. ADS S-parameter simulation (dotted) of 100 mW power amplifier versus measurement (solid).

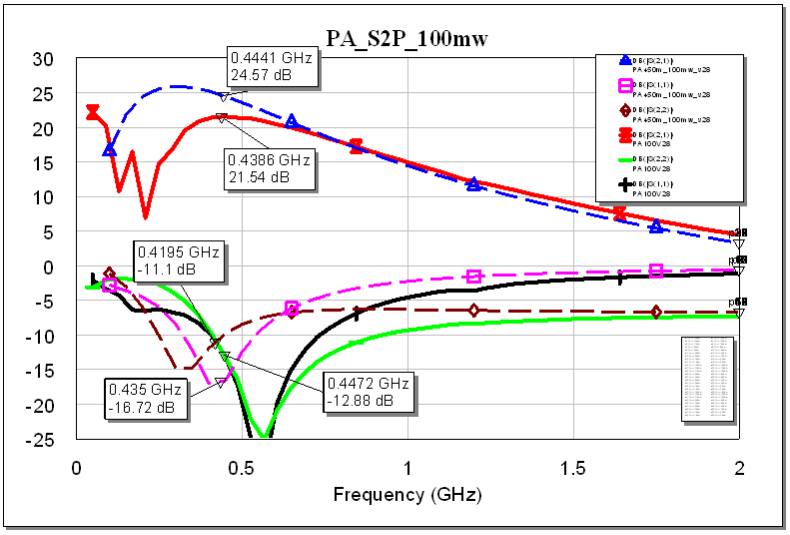

Figure 4. MWO S-parameter simulation (dotted) of 100 mW power amplifier versus measurement (solid).

Simulations for the narrowband low noise amplifier from the test circuit were likewise performed with both simulators for comparison to probe measurements of the GaAs die. Figure 5 shows the s-parameter comparison of measured data to ADS, and figure 6 shows the same versus MWO. Once again, gain was lower than expected but both simulators compare well with measured s-parameter data.

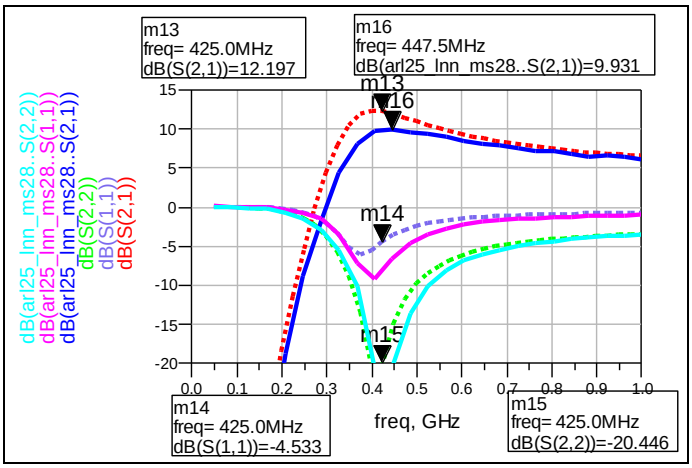

Figure 5. ADS S-parameter simulation (dotted) of narrowband low noise amplifier versus measurement (solid).

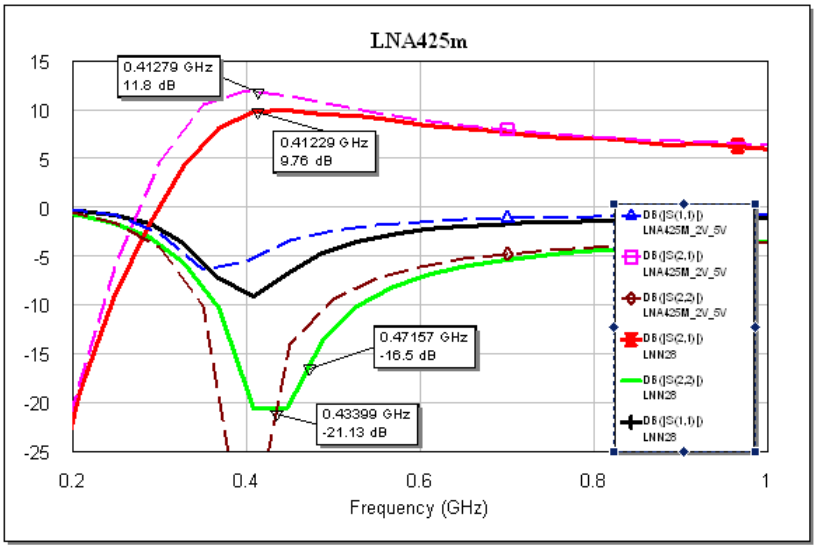

Figure 6. MWO S-parameter simulation (dotted) of narrowband low noise amplifier versus measurement (solid).

The transmit/receive switch was redesigned from the 1st pass to decrease the insertion loss. Large capacitors were needed to provide a positive voltage control for the negative depletion mode PHEMT switches. The tradeoff is the area of the capacitors in the layout versus the insertion loss due to the capacitors. Larger caps reduce the insertion loss but require more space. Additionally, the series and shunt switch devices were doubled in size from the 1st pass design, and care was taken to avoid using the thin lowest level metal0 layer for interconnect. This reduced the 1 dB switch insertion loss of the original design to about 0.4 dB, as measured, in the new design. Only the MWO simulation is compared to probe measurements of the GaAs die. Figure 7 shows the s-parameter comparison of measured data to MWO.

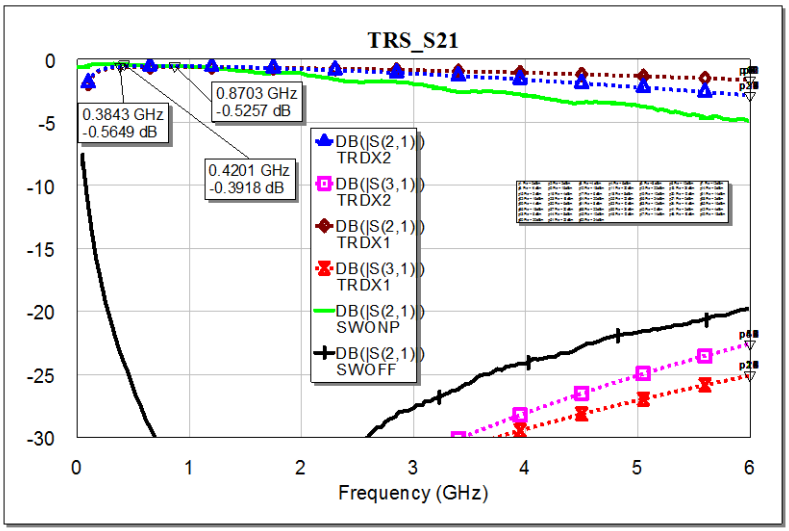

Figure 7. MWO S-parameter simulation (dotted) of TR switch versus measurement (solid).

- ARL21M425—This 425-MHz design contains a BPSK modulator, a 100-mW power amplifier for 2.8 V, a narrowband low DC power consumption low noise amplifier, and a TR switch using positive voltage control inputs with negative threshold depletion PHEMTs.

Simulations for an entire RF front end design were performed in ADS, and include the power amplifier, the BPSK modulator, the low noise amplifier, and the TR switch. Figures 8 and 9 show simulations compared to probe measurements of the GaAs die for the transmit path for both modulator states. Gain is lower than expected for all measured amplifiers in this fabrication run. Figure 10 shows the BPSK phase shift, simulation versus measured, which is very close to the desired 180° over the band 400–550 MHz.

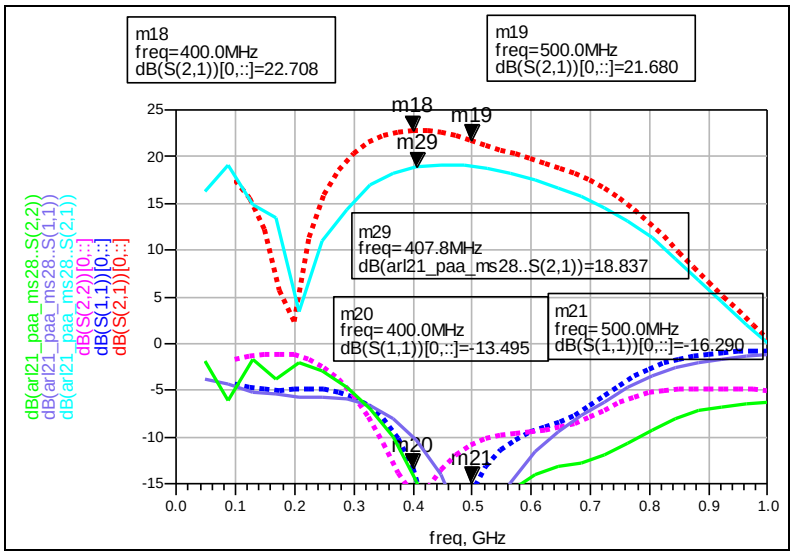

Figure 8. ADS S-parameter simulation (dotted) of ARL21M425 transmit State A versus measurement (solid).

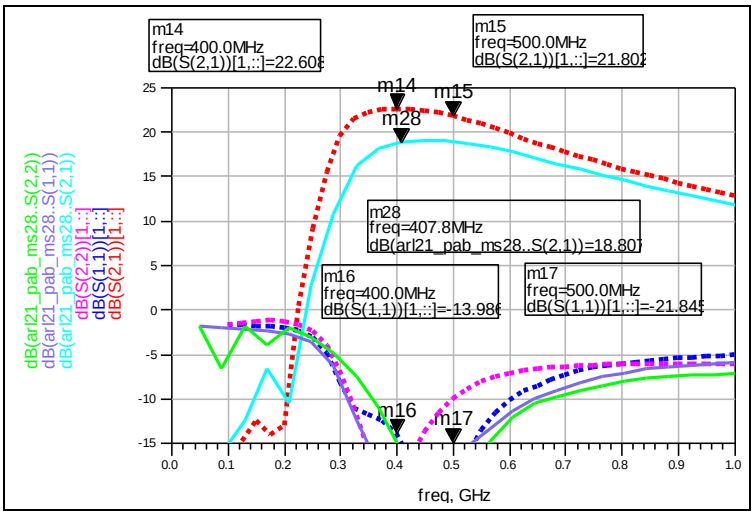

Figure 9. ADS S-parameter simulation (dotted) of ARL21M425 transmit State B versus measurement (solid).

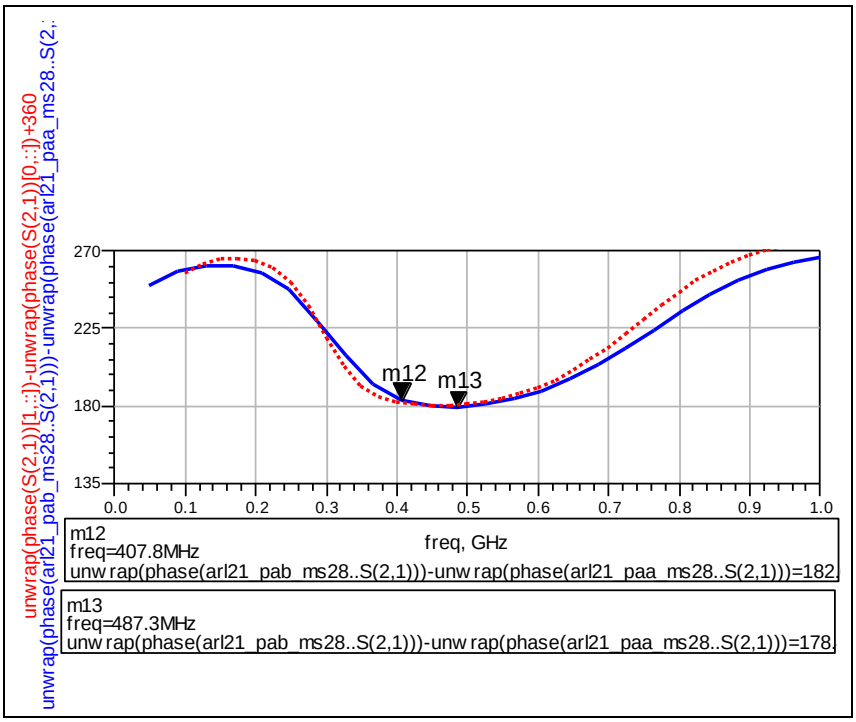

Figure 10. ADS S-parameter simulation (dotted) of ARL21M425 BPSK phase A/B versus measurement (solid).

Simulations for the receive path of the RF front end include the narrowband low noise amplifier and TR switch. Figure 11 shows the s-parameter comparison of measured data to ADS with good agreement, though slightly lower gain.

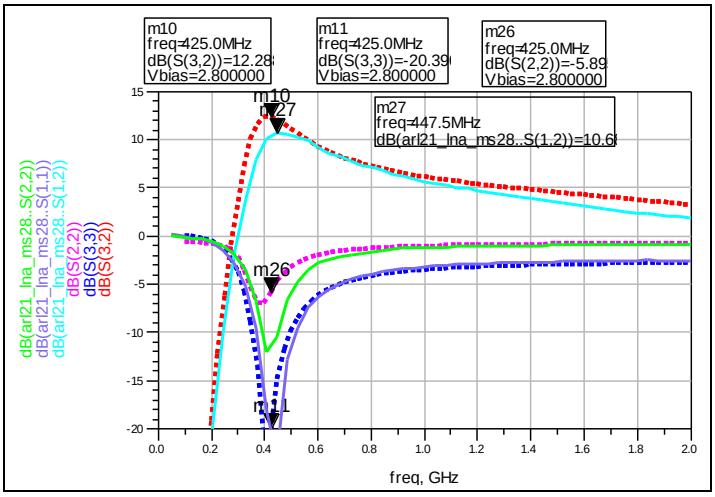

Figure 11. ADS S-parameter simulation (dotted) of ARL21M425 receive path versus measurement (solid).

The isolation provided by the TR switch for the transmit path is shown in figure 12. When the switch is in the receive state, the transmit path is about 48 dB lower. Since the power amplifier

and low noise amplifier have separate power pins, it might be a good idea at the system level to disable power to the amplifier that is not in use. This would save considerable power, especially for the receive mode. The isolation of the receive path is not shown, as it appears that the measurement may have been in error, as it showed 15 dB of isolation rather than the expected 40 dB.

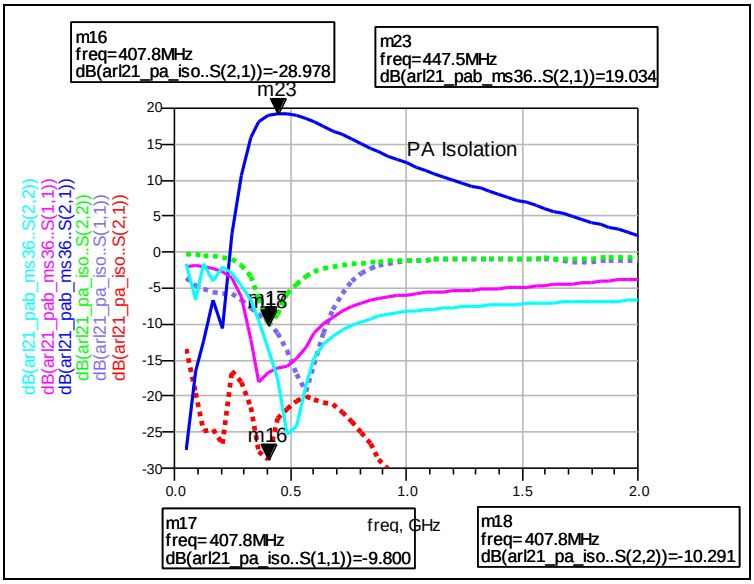

Figure 12. Measured isolation of the transmit path of ARL21M425 (off-dotted, on-solid).

- ARL22M425—This 425-MHz design contains a BPSK modulator, a 50-mW power amplifier for 2.8 V, a narrowband low DC power consumption low noise amplifier, and a TR switch using positive voltage control inputs with negative threshold depletion PHEMTs.

Simulations for an entire RF front end design were performed in ADS, and include the power amplifier, the BPSK modulator, the low noise amplifier, and the TR switch. Figures 13 and 14 show simulations compared to probe measurements of the GaAs die for the transmit path for both modulator states. Gain is lower than expected for all measured amplifiers in this fabrication run. Figure 15 shows the BPSK phase shift simulation versus measured, which is very close to the desired 180° over the band 400–550 MHz.

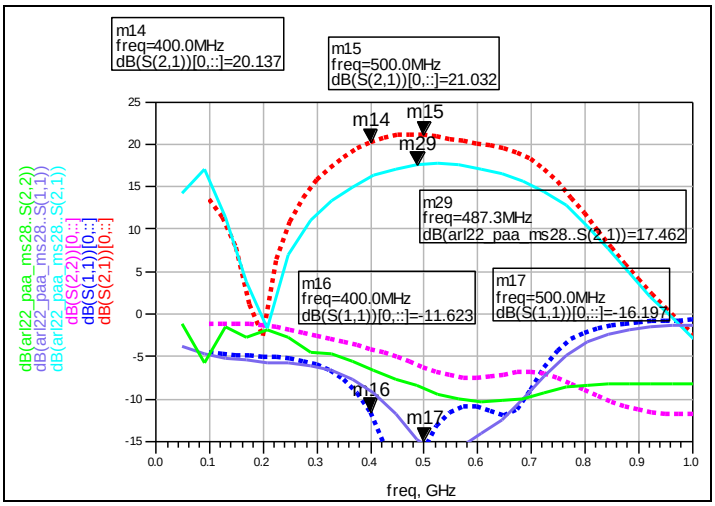

Figure 13. ADS S-parameter simulation (dotted) of ARL22M425 transmit State A versus measurement (solid).

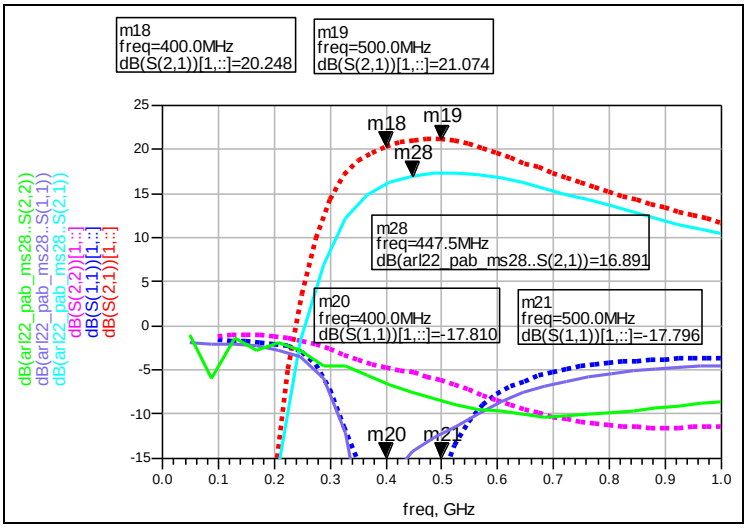

Figure 14. ADS S-parameter simulation (dotted) of ARL22M425 transmit State B versus measurement (solid).

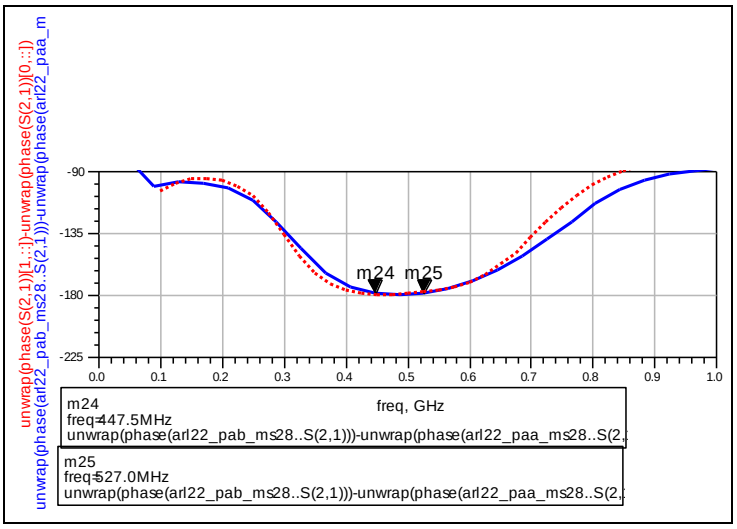

Figure 15. ADS S-parameter simulation (dotted) of ARL22M425 BPSK Phase A/B versus measurement (solid).

Simulations for the receive path of the RF front end include the narrowband low noise amplifier and TR switch. Figure 16 shows the s-parameter comparison of measured data to ADS with good agreement, though slightly lower gain.

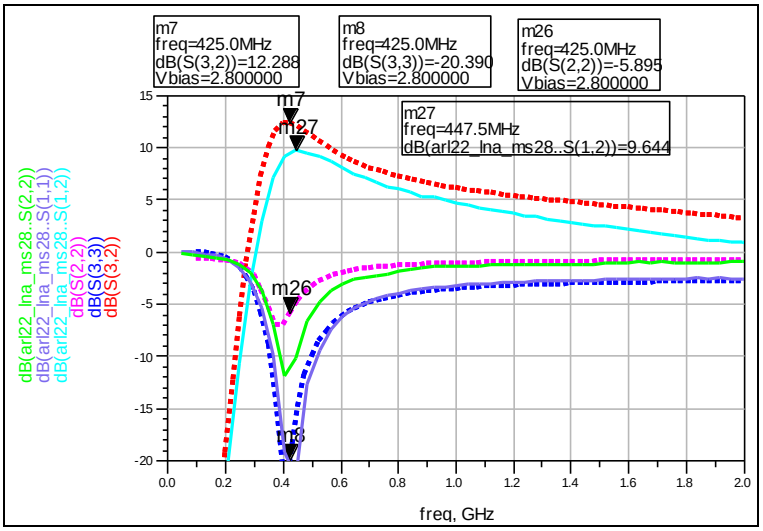

Figure 16. ADS S-parameter simulation (dotted) of ARL22M425 receive path versus measurement (solid).

The isolation provided by the TR switch for the transmit path is shown in figure 17, with the "ON" gain not shown. When the switch is in the receive state, the transmit path is about 46 dB lower. Since the power amplifier and low noise amplifier have separate power pins, it might be a good idea at the system level to disable power to the amplifier that is not in use. This would save considerable power, especially for the receive mode. The isolation of the receive path is shown in figure 18, except for the "ON" state gain, providing about 38 dB of isolation.

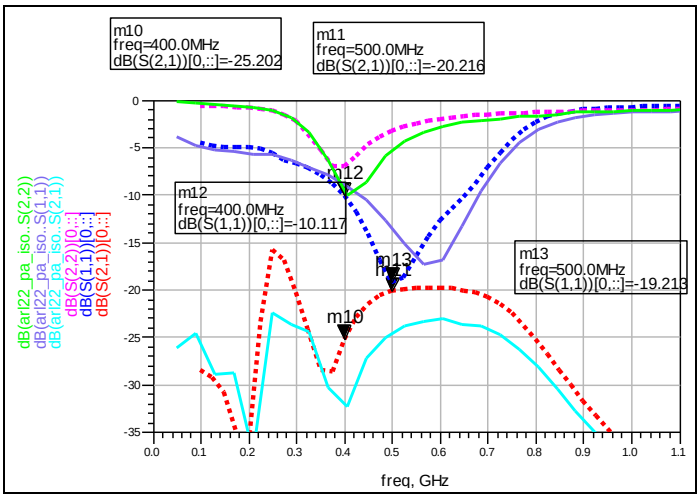

Figure 17. Measured isolation of the transmit path of ARL22M425 (off-dotted, on-solid).

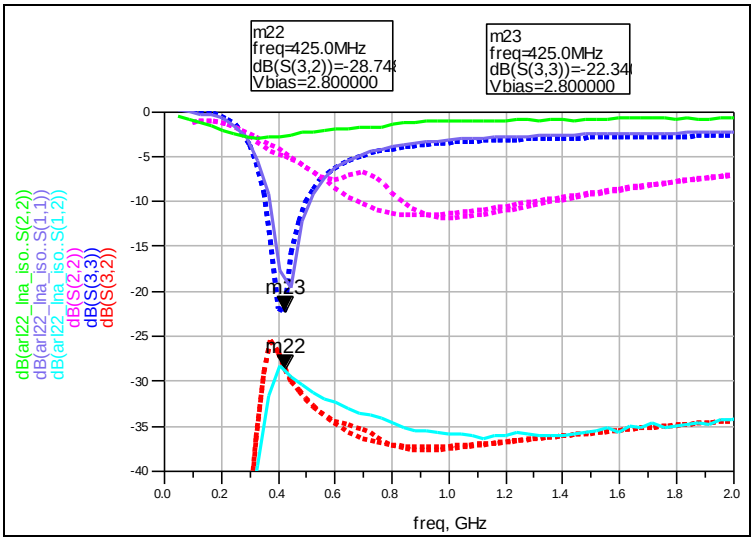

Figure 18. Measured isolation of the receive path of ARL22M425 (off-dotted, on-solid).

- ARL23M425—This 425-MHz design contains a BPSK modulator, a 50/75-mW power amplifier for 2.8/3.6 V, a narrowband low DC power consumption low noise amplifier, and a TR switch using positive voltage control inputs with negative threshold depletion PHEMTs. This design is intended to operate over a broad range of battery voltages.

Simulations for an entire RF front end design were performed in ADS, and include the power amplifier, the BPSK modulator, the low noise amplifier, and the TR switch. This design is intended to operate at 3.6 V, as well as 2.8 V, and uses a broadband power amplifier design from the 1st pass designs. Figures 19 and 20 show simulations compared to probe measurements of the GaAs die for the transmit path for both modulator states. Gain is lower than expected for all

measured amplifiers in this fabrication run. Figure 21 shows the BPSK phase shift simulation versus measured, which is very close to the desired 180° over the band 400–550 MHz.

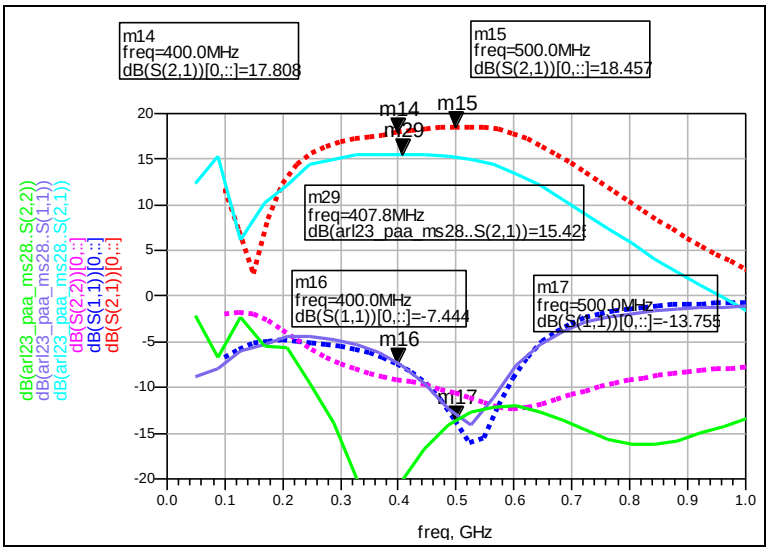

Figure 19. ADS S-parameter simulation (dotted) of ARL23M425 transmit State A versus measurement (solid).

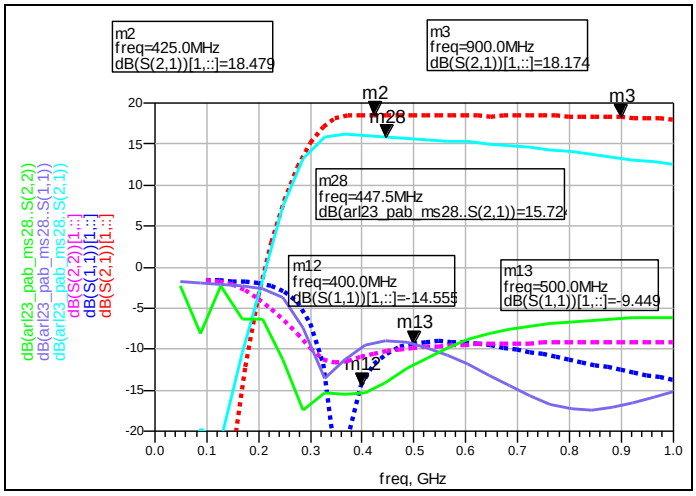

Figure 20. ADS S-parameter simulation (dotted) of ARL23M425 transmit State B versus measurement (solid).

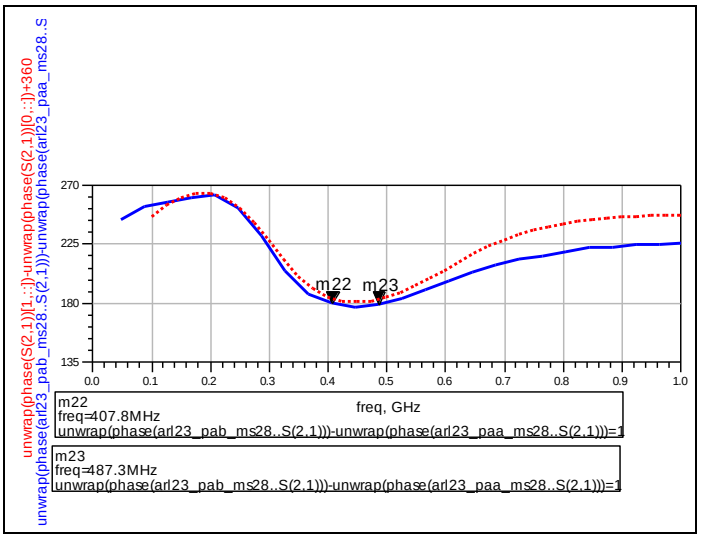

Figure 21. ADS S-parameter simulation (dotted) of ARL23M425 BPSK Phase A/B versus measurement (solid).

Simulations for the receive path of the RF front end include the narrowband low noise amplifier and TR switch. Figure 22 shows the s-parameter comparison of measured data to ADS with good agreement, though slightly lower gain.

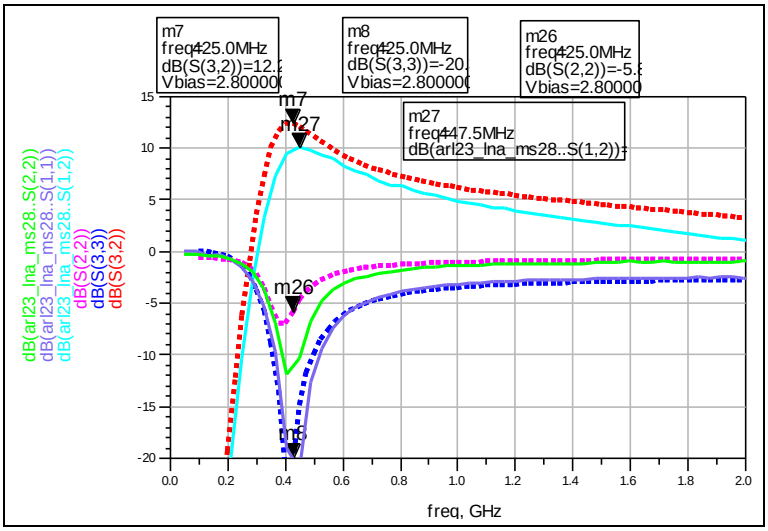

Figure 22. ADS S-parameter simulation (dotted) of ARL23M425 receive path versus measurement (solid).

The isolation provided by the TR switch for the transmit path is shown in figure 23, with the "ON" gain not shown. When the switch is in the receive state, the transmit path is about 42 dB lower. Since the power amplifier and low noise amplifier have separate power pins, it might be a good idea at the system level to disable power to the amplifier not in use. This would save considerable power, especially for the receive mode. The isolation of the receive path is shown in figure 24, except for the "ON" state gain, providing about 36 dB of isolation.

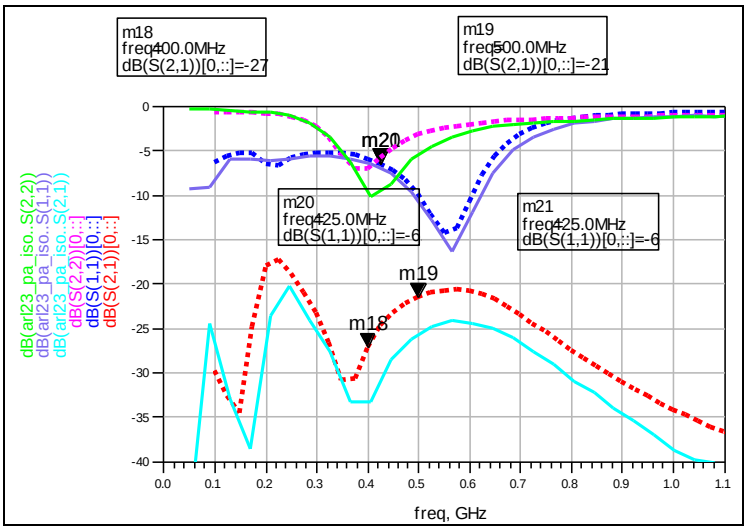

Figure 23. Measured isolation of the transmit path of ARL23M425 (off-dotted, on-solid).

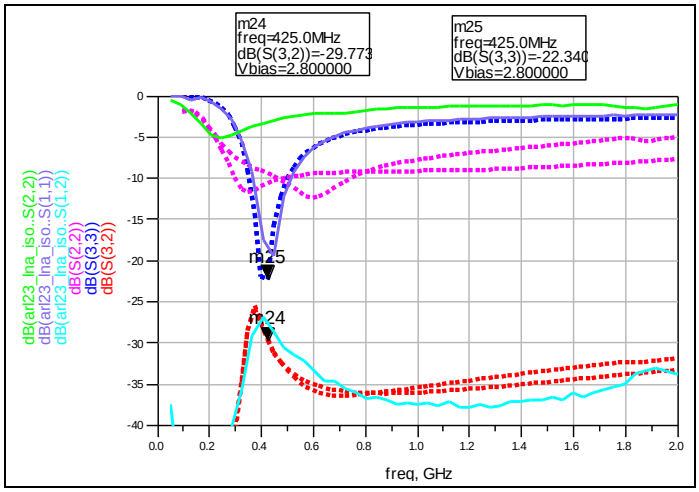

Figure 24. Measured isolation of the receive path of ARL23M425 (off-dotted, on-solid).

- ARL24DB—This dual band design contains a BPSK modulator for 425 or 900 MHz, the broadband 50/75-mW power amplifier for 2.8/3.6 V, a broadband moderate DC power consumption low noise amplifier, and a TR switch using positive voltage control inputs with negative threshold depletion PHEMTs. This design is intended to operate at either the 425 or 900 MHz frequency bands.

Simulations for an entire RF front end design were performed in ADS, and include the power amplifier, the BPSK modulator, the low noise amplifier, and the TR switch. This design is intended to operate around 400 MHz or 900 MHz, as well as 2.8 V or 3.6 V supplies. It uses a broadband power amplifier design and a broadband low noise amplifier from the 1st pass designs. Figures 25 and 26 show simulations compared to probe measurements of the GaAs die for the

transmit path for both modulator states. Gain is lower than expected for all measured amplifiers in this fabrication run. Figure 27 shows the BPSK phase shift simulation versus measured, which is very close to the desired 180° at 400 and 900 MHz.

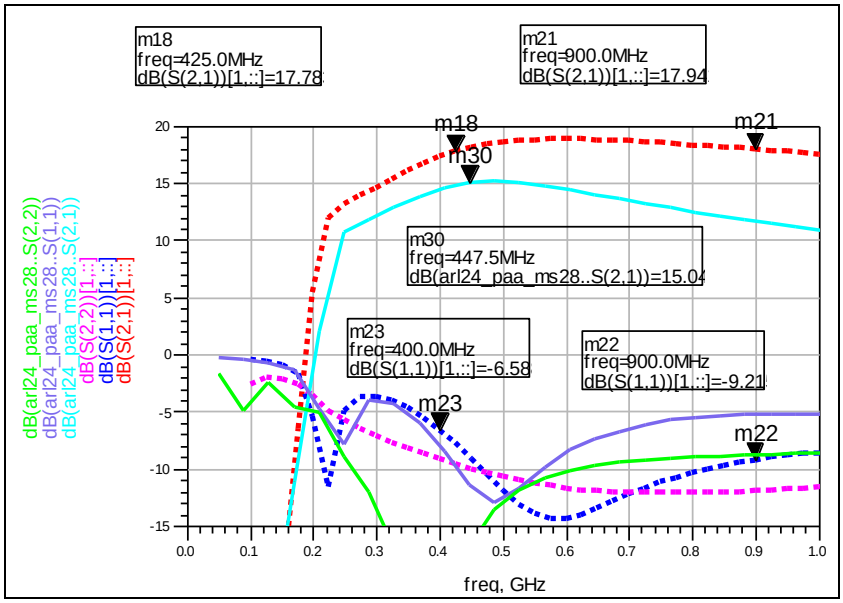

Figure 25. ADS S-parameter simulation (dotted) of ARL24DB transmit State A versus measurement (solid).

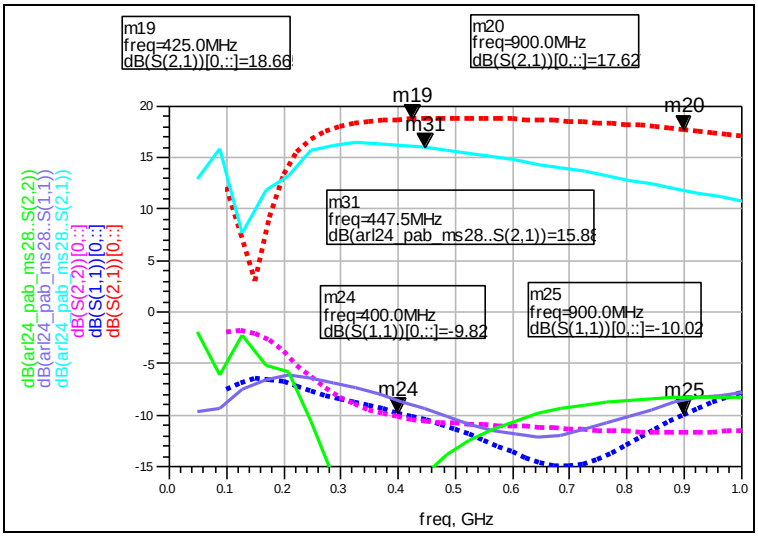

Figure 26. ADS S-parameter simulation (dotted) of ARL24DB transmit State B versus measurement (solid).

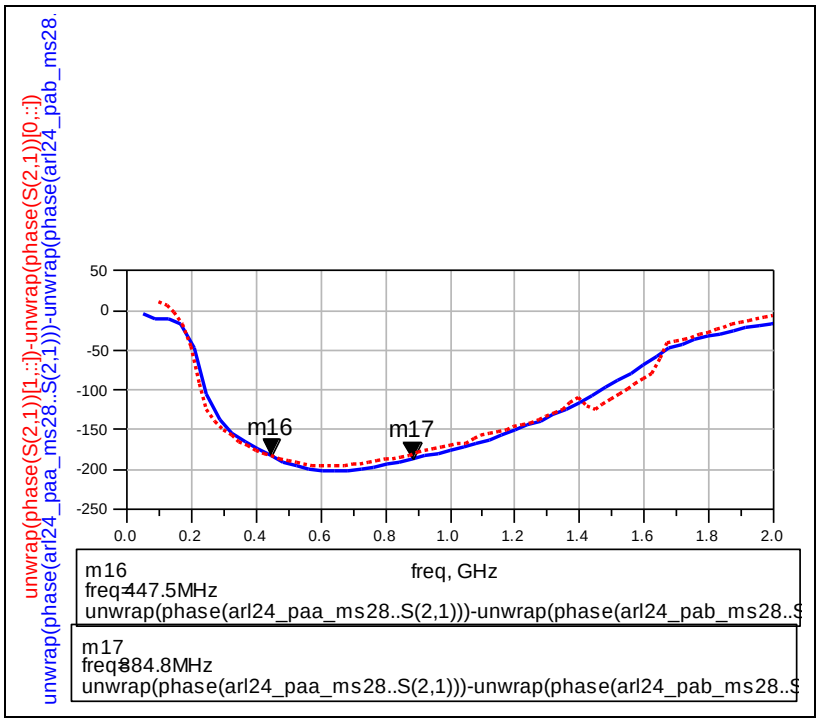

Figure 27. ADS S-parameter simulation (dotted) of ARL24DB BPSK Phase A/B versus measurement (solid).

Simulations for the receive path of the RF front end include the broadband low noise amplifier and TR switch. Figure 28 shows the s-parameter comparison of measured data to ADS with good agreement, though slightly lower gain.

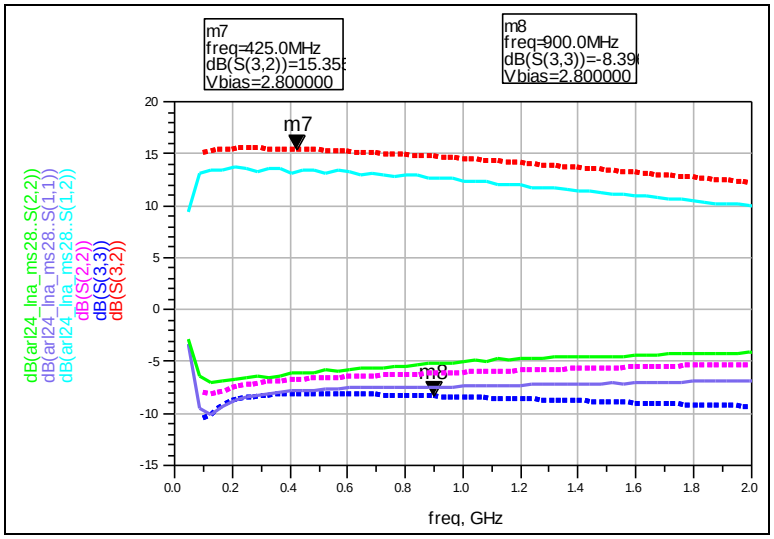

Figure 28. ADS S-parameter simulation (dotted) of ARL24DB receive path versus measurement (solid).

The isolation provided by the TR switch for the transmit path is shown in figure 29, with the "ON" gain not shown. When the switch is in the receive state, the transmit path is about 40 dB lower. Since the power amplifier and low noise amplifier have separate power pins, it might be a good idea at the system level to disable power to the amplifier not being used. This would save considerable power, especially for the receive mode. The isolation of the receive path is shown in figure 30, except for the "ON" state gain, providing about 35 dB of isolation.

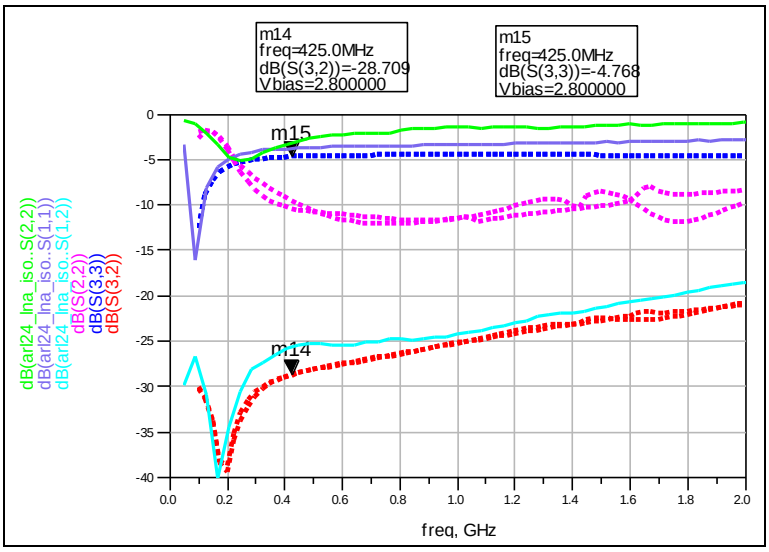

Figure 29. Measured isolation of the transmit path of ARL24DB (off-dotted, on-solid).

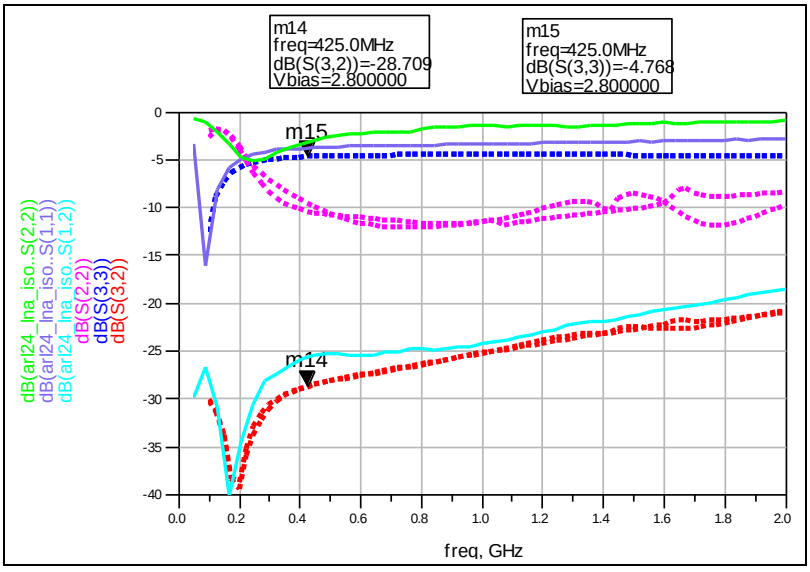

Figure 30. Measured isolation of the receive path of ARL24DB (off-dotted, on-solid).

Performance measurements were also done for the active designs, including noise figure measurements for the receive paths and output power, power compression, and power added

efficiency for the transmit paths or power amplifiers. Efficiencies were much lower than anticipated or hoped. Additional performance measurements will be done with packaged ICs at the board level. It has been noted previously that noise figure measurements at the die level are higher than simulated and could be due to the inability to properly ground or terminate unused inputs. Noise figure measurements as probed are included but are expected to be lower, and closer to simulations, during packaged IC testing.

The performance of the individual test circuits of ARL25 will be shown first, followed by the full RF front end designs (ARL21 to ARL24).

ARL25 contains individual probe testable circuits for the 100 mW power amplifier, the 50 mW power amplifier, a narrowband low noise amplifier, and the TR switch. All of these designs are intended to operate from either 3.0 V batteries or 3.8V li-ion batteries, which are expected to be regulated at a nominal 2.8 V or 3.6 V. Initial measurements of the 100 mW amplifier show that the output power is less than the desired goal of 100 mW with a 2.8 V supply. It is much closer to 100 mW with a 3.6 V supply. This output power exceeds that of the 1st pass designs. Power added efficiency (PAE) is good with 35% achieved at 2.8V and 425 MHz at 0 dBm input power. However, it is less than the desired goal of 45–50% PAE, which was achieved by the 1st pass power amplifier design. Tables 1 and 2 show the performance of the power amplifier with 2.8 V and 3.6 V power supplies, respectively. Figure 31 plots the output power, gain, and PAE of the 100 mW power amplifier at 2.8 V and 3.6 V versus input power.

Table 1. Measured power performance of 100 mW amplifier at 2.8 V and 425 MHz (ARL25).

11/12/2010									
425 MHz	Die#1	**ARL25 PA100mW ARLTILE2 TQPED**				2.8V ; 76 mA			
Pin(SG)	**Pout(SA)**	**Pin(corr)**	**Pout(corr)**	**Gain**	**I1(2.8V)**	**PDC(mw)**	**Pout(mw)**	**Drn Eff**	**PAE**
-15.0	6.67	-15.40	7.07	22.47	76	212.8	5.09	2.4	2.4
-10.0	11.67	-10.40	12.07	22.47	75	210.0	16.11	7.7	7.6
-8.0	13.67	-8.40	14.07	22.47	75	210.0	25.53	12.2	12.1
-6.0	15.17	-6.40	15.57	21.97	74	207.2	36.06	17.4	17.3
-4.0	16.50	-4.40	16.90	21.30	72	201.6	48.98	24.3	24.1
-2.0	17.33	-2.40	17.73	20.13	69	193.2	59.29	30.7	30.4
0.0	17.83	-0.40	18.23	18.63	67	187.6	66.53	35.5	35.0

Table 2. Measured power performance of 100 mW amplifier at 3.6 V and 425 MHz (ARL25).

425 MHz	Die#1	**ARL25 PA100mW ARLTILE2 TQPED**				3.6V ; 79 mA			
Pin(SG)	**Pout(SA)**	**Pin(corr)**	**Pout(corr)**	**Gain**	**I1(3.6V)**	**PDC(mw)**	**Pout(mw)**	**Drn Eff**	**PAE**
-15.0	6.50	-15.40	6.90	22.30	79	284.4	4.90	1.7	1.7
-10.0	11.50	-10.40	11.90	22.30	79	284.4	15.49	5.4	5.4
-8.0	13.50	-8.40	13.90	22.30	79	284.4	24.55	8.6	8.6
-6.0	15.50	-6.40	15.90	22.30	79	284.4	38.90	13.7	13.6
-4.0	17.17	-4.40	17.57	21.97	78	280.8	57.15	20.4	20.2
-2.0	18.33	-2.40	18.73	21.13	78	280.8	74.64	26.6	26.4
0.0	19.00	-0.40	19.40	19.80	77	277.2	87.10	31.4	31.1
2.0	19.33	1.60	19.73	18.13	76	273.6	93.97	34.3	33.8

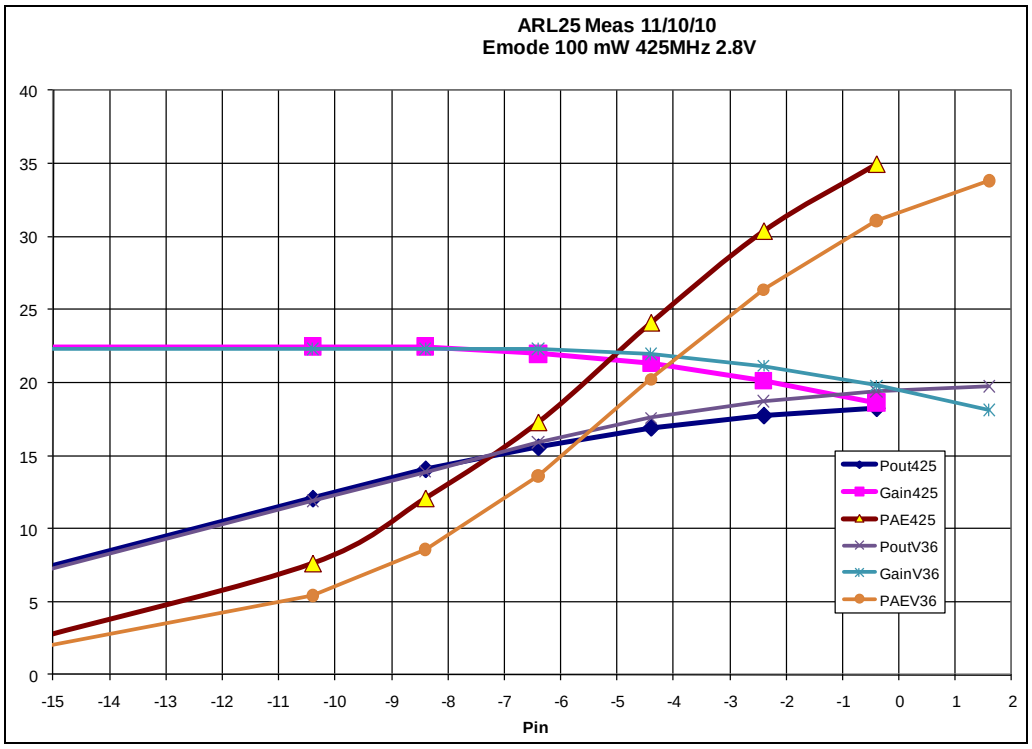

Figure 31. Plot of measured power performance of 100 mW amplifier at 2.8/3.6 V and 425 MHz (ARL25).

Initial measurements of the 50 mW amplifier show that the output power is less than the desired goal using a 2.8 V supply. However, the output power is approximately 50 mW with a 3.6 V supply. The PAE is less than the desired goal of 45–50% PAE, which was achieved by the 1st pass power amplifier design. Tables 3 and 4 show the performance of the power amplifier at 425 MHz with 2.8 V and 3.6 V power supplies, respectively. Figure 32 plots the output power, gain, and PAE of the 50 mW power amplifier at 2.8 V and 3.6 V versus input power at 425 MHz. Performance was slightly better at 500 MHz as shown in tables 5, 6, and 7 taken at 2.5 V, 2.8 V, and 3.6 V. Figure 33 plots the output power, gain, and PAE of the 50 mW power amplifier at 2.5 V, 2.8 V, and 3.6 V versus input power at 500 MHz. The output power exceeds 60 mW at 3.6 V, with good PAE of approximately 35% for 2.5 V to 3.6 V supply voltages.

Table 3. Measured power performance of 50 mW amplifier at 2.8 V and 425 MHz (ARL25).

11/12/2010									
425 MHz	Die#1	**ARL25 PA50mW ARLTILE2 TQPED**				2.8V ; 38 mA			
Pin(SG)	**Pout(SA)**	**Pin(corr)**	**Pout(corr)**	**Gain**	**I1(2.8V)**	**PDC(mw)**	**Pout(mw)**	**Drn Eff**	**PAE**
-15.0	3.83	-15.40	4.23	19.63	38	106.4	2.65	2.5	2.5
-10.0	8.83	-10.40	9.23	19.63	39	109.2	8.38	7.7	7.6
-8.0	10.67	-8.40	11.07	19.47	40	112.0	12.79	11.4	11.3
-6.0	12.50	-6.40	12.90	19.30	41	114.8	19.50	17.0	16.8
-4.0	14.00	-4.40	14.40	18.80	43	120.4	27.54	22.9	22.6
-2.0	14.83	-2.40	15.23	17.63	44	123.2	33.34	27.1	26.6
0.0	15.33	-0.40	15.73	16.13	45	126.0	37.41	29.7	29.0

Table 4. Measured power performance of 50 mW amplifier at 3.6 V and 425 MHz (ARL25).

425 MHz	Die#1	ARL25 PA50mW ARLTILE2 TQPED				3.6V ; 40 mA			
Pin(SG)	**Pout(SA)**	**Pin(corr)**	**Pout(corr)**	**Gain**	**I1(3.6V)**	**PDC(mw)**	**Pout(mw)**	**Drn Eff**	**PAE**
-15.0	3.83	-15.40	4.23	19.63	41	147.6	2.65	1.8	1.8
-10.0	8.67	-10.40	9.07	19.47	41	147.6	8.07	5.5	5.4
-8.0	10.67	-8.40	11.07	19.47	42	151.2	12.79	8.5	8.4
-6.0	12.50	-6.40	12.90	19.30	43	154.8	19.50	12.6	12.4
-4.0	14.00	-4.40	14.40	18.80	45	162.0	27.54	17.0	16.8
-2.0	15.50	-2.40	15.90	18.30	48	172.8	38.90	22.5	22.2
0.0	16.50	-0.40	16.90	17.30	50	180.0	48.98	27.2	26.7

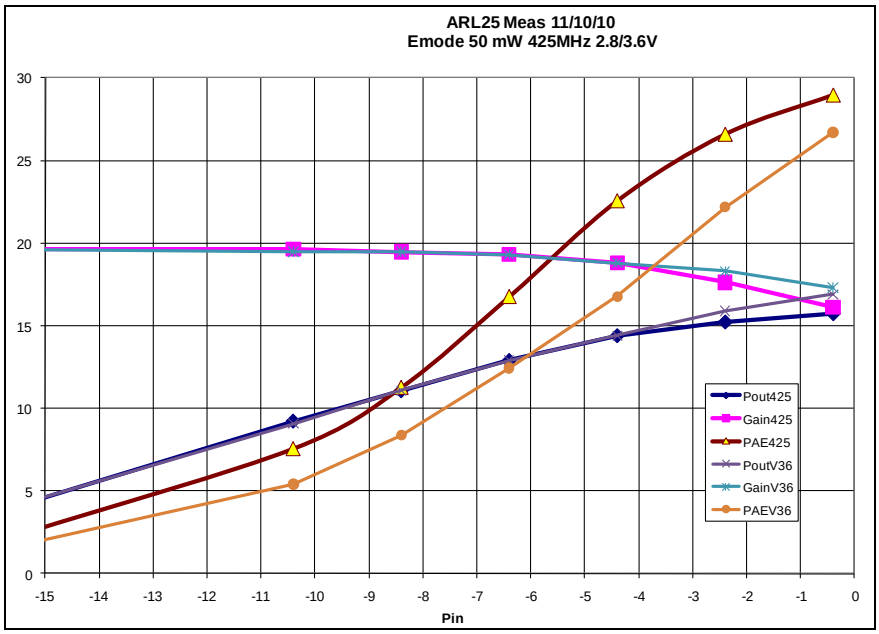

Figure 32. Plot of measured power performance of 50 mW amplifier at 2.8/3.6 V and 425 MHz (ARL25).

Table 5. Measured power performance of 50 mW amplifier at 2.5 V and 500 MHz (ARL25).

11/23/2010	Re-Measured								
500 MHz	Die#1	ARL25 PA50mW ARLTILE2 TQPED				2.5V ; 38 mA			
Pin(SG)	**Pout(SA)**	**Pin(corr)**	**Pout(corr)**	**Gain**	**I1(2.5V)**	**PDC(mw)**	**Pout(mw)**	**Drn Eff**	**PAE**
-15	5.67	-15.35	6.02	21.37	38	95.0	4.00	4.2	4.2
-10	10.17	-10.35	10.52	20.87	38	95.0	11.27	11.9	11.8
-8	12.00	-8.35	12.35	20.70	39	97.5	17.18	17.6	17.5
-6	13.50	-6.35	13.85	20.20	40	100.0	24.27	24.3	24.0
-5	14.17	-5.35	14.52	19.87	40	100.0	28.31	28.3	28.0
-4	14.67	-4.35	15.02	19.37	40	100.0	31.77	31.8	31.4
-3	15.00	-3.35	15.35	18.70	40	100.0	34.28	34.3	33.8
-2	15.17	-2.35	15.52	17.87	40	100.0	35.65	35.6	35.1

Table 6. Measured power performance of 50 mW amplifier at 2.8 V and 500 MHz (ARL25).

500 MHz	Die#1	ARL25 PA50mW ARLTILE2 TQPED				2.8V ; 38 mA			
Pin(SG)	**Pout(SA)**	**Pin(corr)**	**Pout(corr)**	**Gain**	**I1(2.8V)**	**PDC(mw)**	**Pout(mw)**	**Drn Eff**	**PAE**
-15	5.67	-15.40	6.07	21.47	38	106.4	4.05	3.8	3.8
-10	10.17	-10.40	10.57	20.97	39	109.2	11.40	10.4	10.4
-8	12.00	-8.40	12.40	20.80	39	109.2	17.38	15.9	15.8
-6	13.67	-6.40	14.07	20.47	40	112.0	25.53	22.8	22.6
-5	14.33	-5.40	14.73	20.13	41	114.8	29.72	25.9	25.6
-4	14.83	-4.40	15.23	19.63	41	114.8	33.34	29.0	28.7
-3	15.17	-3.40	15.57	18.97	41	114.8	36.06	31.4	31.0
-2	15.50	-2.40	15.90	18.30	42	117.6	38.90	33.1	32.6
-1	15.67	-1.40	16.07	17.47	42	117.6	40.46	34.4	33.8

Table 7. Measured power performance of 50 mW amplifier at 3.6 V and 500 MHz (ARL25).

500 MHz	Die#1	ARL25 PA50mW ARLTILE2 TQPED				3.6V ; 41 mA			
Pin(SG)	**Pout(SA)**	**Pin(corr)**	**Pout(corr)**	**Gain**	**I1(3.6V)**	**PDC(mw)**	**Pout(mw)**	**Drn Eff**	**PAE**
-15	5.50	-15.40	5.90	21.30	41	147.6	3.89	2.6	2.6
-10	10.00	-10.40	10.40	20.80	41	147.6	10.96	7.4	7.4
-8	11.83	-8.40	12.23	20.63	41	147.6	16.71	11.3	11.2
-6	13.67	-6.40	14.07	20.47	42	151.2	25.53	16.9	16.7
-5	14.50	-5.40	14.90	20.30	43	154.8	30.90	20.0	19.8
-4	15.33	-4.40	15.73	20.13	44	158.4	37.41	23.6	23.4
-3	16.17	-3.40	16.57	19.97	45	162.0	45.39	28.0	27.7
-2	16.83	-2.40	17.23	19.63	46	165.6	52.84	31.9	31.6
-1	17.17	-1.40	17.57	18.97	47	169.2	57.15	33.8	33.3
0	17.50	-0.40	17.90	18.30	48	172.8	61.66	35.7	35.2

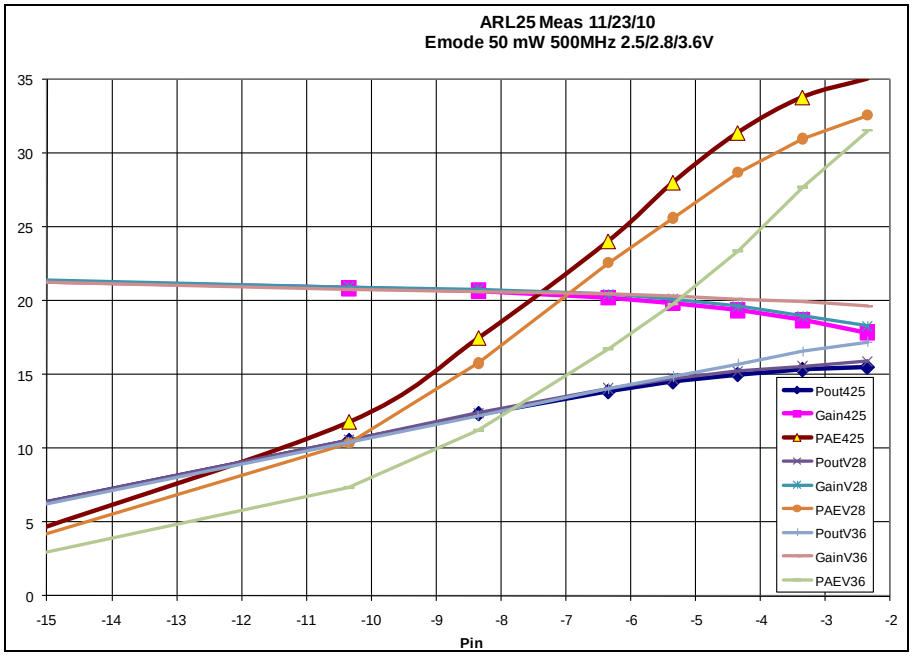

Figure 33. Plot of measured power performance of 50 mW amplifier at 2.5/2.8/3.6 V and 500 MHz (ARL25).

Figure 34 shows the measured performance of the narrowband low noise amplifier at 2.8 V where the "raw" lines show gain and noise figure including setup cable losses, and the "corr" lines show the true gain and noise figure. Measurements of the narrowband low noise amplifier show a good noise figure just above 2 dB at 425 MHz (yellow line in figure 34). The low DC power consumption was measured as 3 mA and was very constant over the supply voltages of 2.8 V and 3.6 V, as expected. Gain (cyan line in figure 34) was about 11 dB as measured with the noise figure meter, which is consistent with the s-parameter measurements.

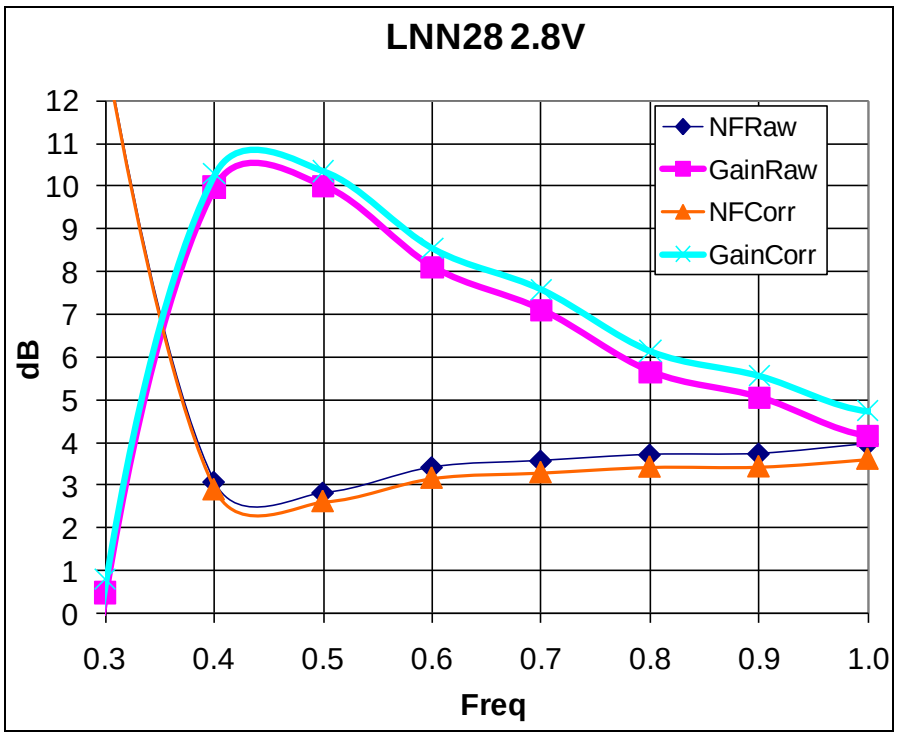

Figure 34. Plot of noise figure (yellow) and gain (cyan) of narrowband low noise amplifier at 2.8 V (ARL25).

ARL21M425 is a front end RF IC containing a BPSK modulator, the 100 mW power amplifier, the narrowband low noise amplifier, and the TR switch. Tables 8 and 9 show the performance of the transmit path including the modulator, power amplifier, and TR switch with 2.8 V and 3.6 V power supplies, respectively. Figure 35 plots the output power, gain, and PAE of the transmit path at 2.8 V and 3.6 V versus input power. Figure 36 shows the measured performance of the receive path, which includes a narrowband low noise amplifier and the TR switch at 3.6 V, where the "raw" lines show gain and noise figure including setup cable losses; and the "corr" lines show the true gain and noise figure. Past probe tests of noise figure of the RF front end IC show a higher than expected noise figure, which could be due to allowing some of the TR switch control inputs to "float" to 0 V due to the limited number of DC needle probes available. Testing at the packaged part level with all control inputs properly terminated is expected to show a significant improvement in the noise figure, probably a dB or more. Gain (cyan line in figure

36) was about 11 dB as measured with the noise figure meter and includes the expected TR switch insertion loss of about 0.5 dB.

Table 8. Measured power performance of ARL21M425 at 2.8 V and 425 MHz.

11/10/2010									
425 MHz	Die#1	**ARL21M425 ARLTILE2 TQPED**				2.8V ; 68 mA			
Pin(SG)	**Pout(SA)**	**Pin(corr)**	**Pout(corr)**	**Gain**	**I1(2.8V)**	**PDC(mw)**	**Pout(mw)**	**Drn Eff**	**PAE**
-15.0	3.74	-15.40	4.14	19.54	68	190.4	2.59	1.4	1.3
-10.0	8.36	-10.40	8.76	19.16	68	190.4	7.52	3.9	3.9
-8.0	10.25	-8.40	10.65	19.05	67	187.6	11.61	6.2	6.1
-6.0	11.96	-6.40	12.36	18.76	67	187.6	17.22	9.2	9.1
-4.0	13.26	-4.40	13.66	18.06	66	184.8	23.23	12.6	12.4
-2.0	14.16	-2.40	14.56	16.96	65	182.0	28.58	15.7	15.4
0.0	14.74	-0.40	15.14	15.54	63	176.4	32.66	18.5	18.0

Table 9. Measured power performance of ARL21M425 at 3.6 V and 425 MHz.

425 MHz	Die#1	**ARL21M425 ARLTILE2 TQPED**				3.6V ; 73 mA			
Pin(SG)	**Pout(SA)**	**Pin(corr)**	**Pout(corr)**	**Gain**	**I1(3.6V)**	**PDC(mw)**	**Pout(mw)**	**Drn Eff**	**PAE**
-15.0	3.74	-15.40	4.14	19.54	73	262.8	2.59	1.0	1.0
-10.0	8.13	-10.40	8.53	18.93	72	259.2	7.13	2.8	2.7
-8.0	10.33	-8.40	10.73	19.13	72	259.2	11.83	4.6	4.5
-6.0	12.02	-6.40	12.42	18.82	72	259.2	17.46	6.7	6.6
-4.0	13.42	-4.40	13.82	18.22	72	259.2	24.10	9.3	9.2
-2.0	14.42	-2.40	14.82	17.22	73	262.8	30.34	11.5	11.3
0.0	15.26	-0.40	15.66	16.06	75	270.0	36.81	13.6	13.3
2.0	15.86	1.60	16.26	14.66	78	280.8	42.27	15.1	14.5

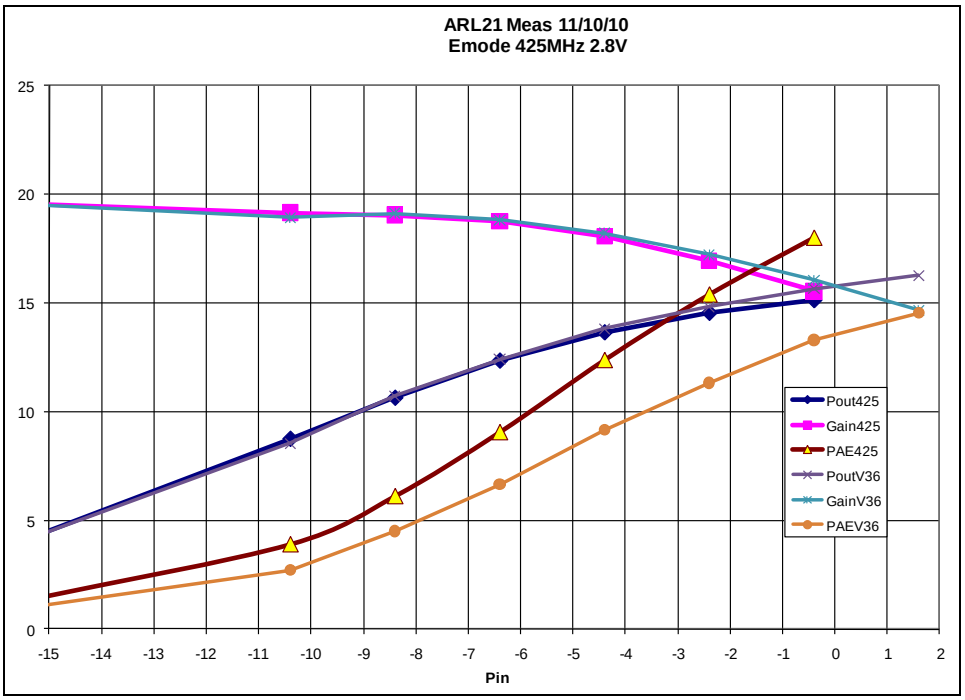

Figure 35. Plot of measured power performance of ARL21M425 at 2.8/3.6 V and 425 MHz.

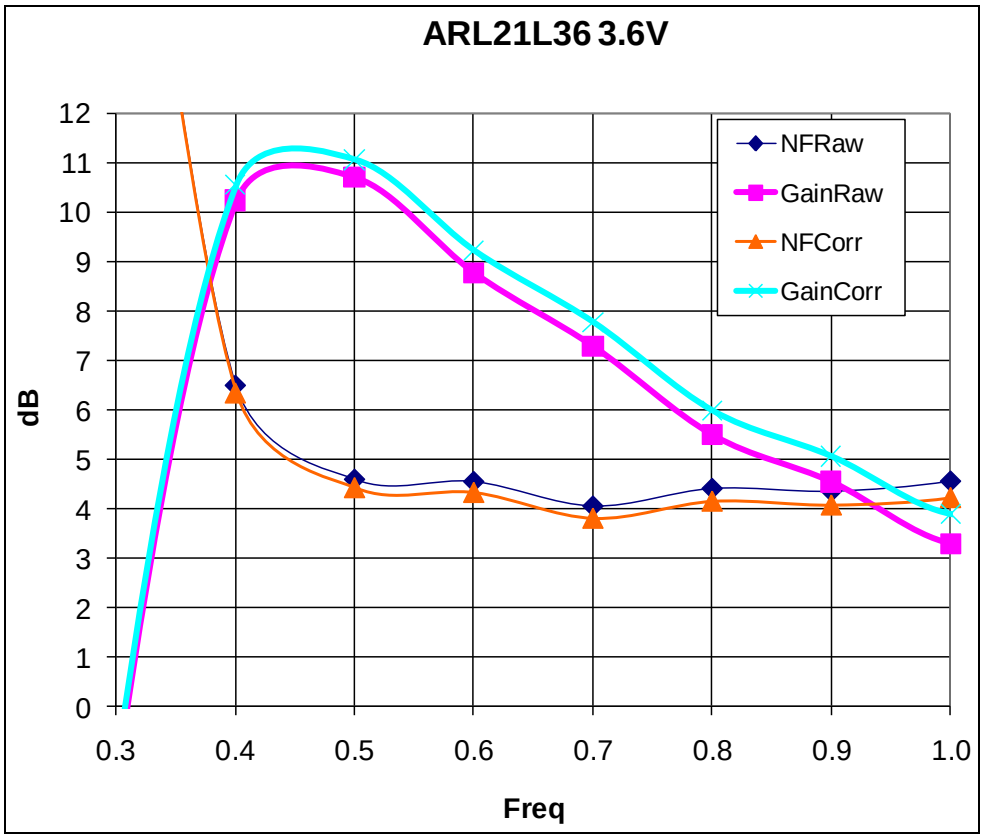

Figure 36. Plot of noise figure (yellow) and gain (cyan) of ARL21M425 at 3.6 V.

ARL22M425 is a front end RF IC containing a BPSK modulator, the 50 mW power amplifier, the narrowband low noise amplifier, and the TR switch. Tables 10 and 11 show the performance of the transmit path including the modulator, power amplifier, and TR switch with 2.8 V and 3.6 V power supplies, respectively. Figure 37 plots the output power, gain, and PAE of the transmit path at 2.8 V and 3.6 V versus input power. Figure 38 shows the measured performance of the receive path, which includes a narrowband low noise amplifier and the TR switch at 3.6 V, where the "raw" lines show gain and noise figure including setup cable losses, and the "corr" lines show the true gain and noise figure. Past probe tests of the noise figure of the RF front end IC show a higher than expected noise figure, which might be due to allowing some of the TR switch control inputs to "float" to 0 V due to the limited number of DC needle probes available. Testing at the packaged part level with all control inputs properly terminated is expected to show a significant improvement in the noise figure, probably a dB or more. Gain (cyan line in figure 38) was about 10.5 dB as measured with the noise figure meter, which is comparable to the individual LNA measurement of ARL25 minus the TR switch insertion loss of about 0.5 dB.

Table 10. Measured power performance of ARL22M425 at 2.8 V and 425 MHz.

11/12/2010									
425 MHz	Die#1	**ARL22M425 ARLTILE2 TQPED**				2.8V ; 39 mA			
Pin(SG)	**Pout(SA)**	**Pin(corr)**	**Pout(corr)**	**Gain**	**I1(2.8V)**	**PDC(mw)**	**Pout(mw)**	**Drn Eff**	**PAE**
-15.0	1.83	-15.40	2.23	17.63	39	109.2	1.67	1.5	1.5
-10.0	6.67	-10.40	7.07	17.47	39	109.2	5.09	4.7	4.6
-8.0	8.67	-8.40	9.07	17.47	39	109.2	8.07	7.4	7.3
-6.0	10.50	-6.40	10.90	17.30	40	112.0	12.30	11.0	10.8
-4.0	12.00	-4.40	12.40	16.80	40	112.0	17.38	15.5	15.2
-2.0	13.33	-2.40	13.73	16.13	42	117.6	23.60	20.1	19.6
0.0	14.17	-0.40	14.57	14.97	44	123.2	28.64	23.2	22.5
2.0	14.50	1.60	14.90	13.30	46	128.8	30.90	24.0	22.9

Table 11. Measured power performance of ARL22M425 at 3.6 V and 425 MHz.

425 MHz	Die#1	**ARL22M425 ARLTILE2 TQPED**				3.6V ; 41 mA			
Pin(SG)	**Pout(SA)**	**Pin(corr)**	**Pout(corr)**	**Gain**	**I1(3.6V)**	**PDC(mw)**	**Pout(mw)**	**Drn Eff**	**PAE**
-15.0	1.67	-15.40	2.07	17.47	41	147.6	1.61	1.1	1.1
-10.0	6.50	-10.40	6.90	17.30	41	147.6	4.90	3.3	3.3
-8.0	8.50	-8.40	8.90	17.30	41	147.6	7.76	5.3	5.2
-6.0	10.33	-6.40	10.73	17.13	42	151.2	11.83	7.8	7.7
-4.0	12.00	-4.40	12.40	16.80	42	151.2	17.38	11.5	11.3
-2.0	13.17	-2.40	13.57	15.97	44	158.4	22.75	14.4	14.0
0.0	14.17	-0.40	14.57	14.97	47	169.2	28.64	16.9	16.4
2.0	15.00	1.60	15.40	13.80	50	180.0	34.67	19.3	18.5

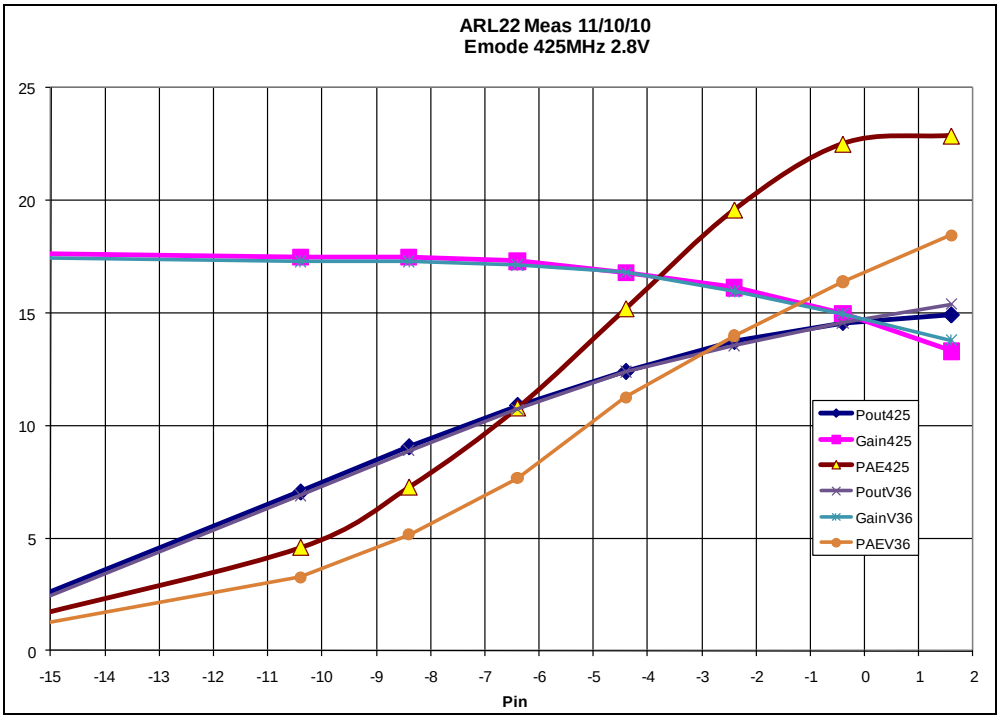

Figure 37. Plot of measured power performance of ARL22M425 at 2.8/3.6 V and 425 MHz.

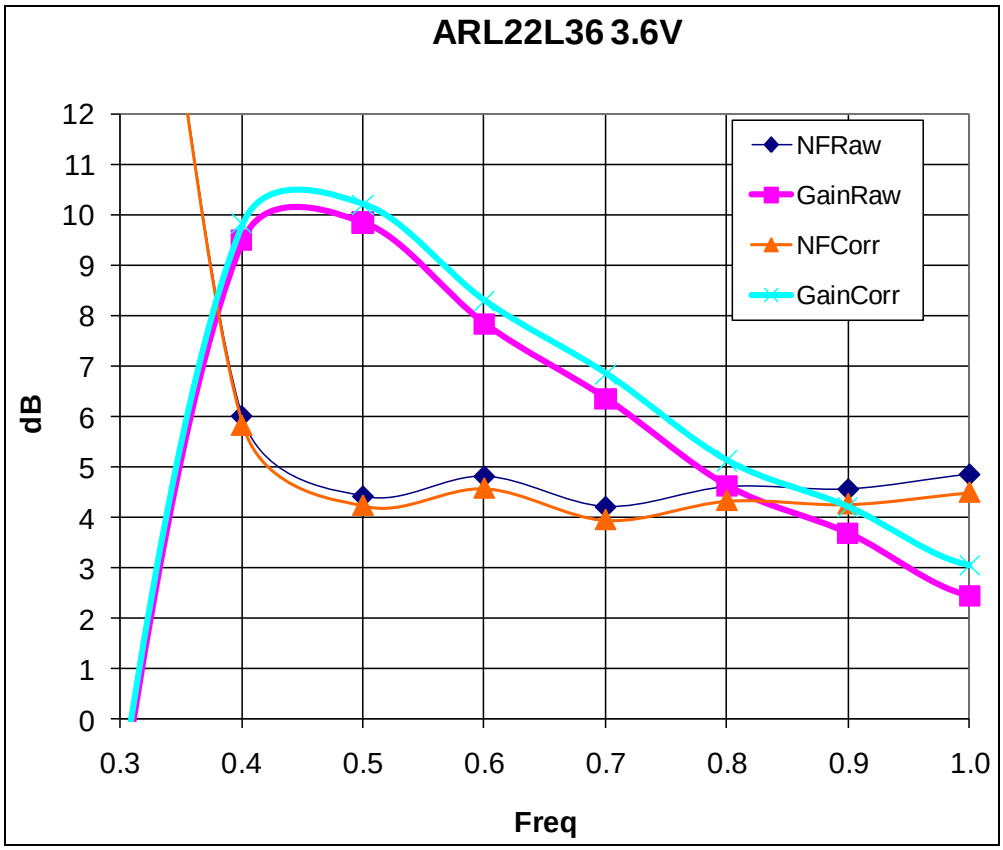

Figure 38. Plot of noise figure (yellow) and Gain (cyan) of ARL22M425 at 3.6 V.

ARL23M425 is a front end RF IC containing a BPSK modulator, a broadband power amplifier based on the 1st pass designs, the narrowband low noise amplifier, and the TR switch. Tables 12 and 13 show the performance of the transmit path including the modulator, power amplifier, and TR switch with 2.8 V and 3.6 V power supplies, respectively. Figure 39 plots the output power, gain, and PAE of the transmit path at 2.8 V and 3.6 V versus input power. Figure 40 shows the measured performance of the receive path, which includes a narrowband low noise amplifier and the TR switch at 3.6 V, where the "raw" lines show gain and noise figure including setup cable losses, and the "corr" lines show the true gain and noise figure. Past probe tests of the noise figure of the RF front end IC show a higher than expected noise figure, which might be due to allowing some of the TR switch control inputs to "float" to 0 V due to the limited number of DC needle probes available. Testing at the packaged part level with all control inputs properly terminated is expected to show a significant improvement in the noise figure, probably a dB or more. Gain (cyan line in figure 40) was about 10.5 dB as measured with the noise figure meter, which is comparable to the individual LNA measurement of ARL25 minus the TR switch insertion loss of about 0.5 dB.

Table 12. Measured power performance of ARL23M425 at 2.8 V and 425 MHz.

	11/10/2010								
425 MHz	Die#1	**ARL23M425 ARLTILE2 TQPED**				2.8V ; 38 mA			
Pin(SG)	**Pout(SA)**	**Pin(corr)**	**Pout(corr)**	**Gain**	**I1(2.8V)**	**PDC(mw)**	**Pout(mw)**	**Drn Eff**	**PAE**
-15.0	-0.28	-15.40	0.12	15.52	38	106.4	1.03	1.0	0.9
-10.0	5.12	-10.40	5.52	15.92	38	106.4	3.56	3.4	3.3
-8.0	7.26	-8.40	7.66	16.06	37	103.6	5.83	5.6	5.5
-6.0	8.80	-6.40	9.20	15.60	37	103.6	8.32	8.0	7.8
-4.0	10.16	-4.40	10.56	14.96	36	100.8	11.38	11.3	10.9
-2.0	11.15	-2.40	11.55	13.95	35	98.0	14.29	14.6	14.0
0.0	11.72	-0.40	12.12	12.52	34	95.2	16.29	17.1	16.2
2.0	12.06	1.60	12.46	10.86	32	89.6	17.62	19.7	18.1

Table 13. Measured power performance of ARL23M425 at 3.6 V and 425 MHz.

425 MHz	Die#1	**ARL23M425 ARLTILE2 TQPED**				3.6V ; 40 mA			
Pin(SG)	**Pout(SA)**	**Pin(corr)**	**Pout(corr)**	**Gain**	**I1(3.6V)**	**PDC(mw)**	**Pout(mw)**	**Drn Eff**	**PAE**
-15.0	0.80	-15.40	1.20	16.60	40	144.0	1.32	0.9	0.9
-10.0	5.46	-10.40	5.86	16.26	40	144.0	3.85	2.7	2.6
-8.0	7.31	-8.40	7.71	16.11	39	140.4	5.90	4.2	4.1
-6.0	8.97	-6.40	9.37	15.77	39	140.4	8.65	6.2	6.0
-4.0	10.32	-4.40	10.72	15.12	39	140.4	11.80	8.4	8.1
-2.0	11.35	-2.40	11.75	14.15	39	140.4	14.96	10.7	10.2
0.0	12.10	-0.40	12.50	12.90	38	136.8	17.78	13.0	12.3
2.0	12.52	1.60	12.92	11.32	38	136.8	19.59	14.3	13.3

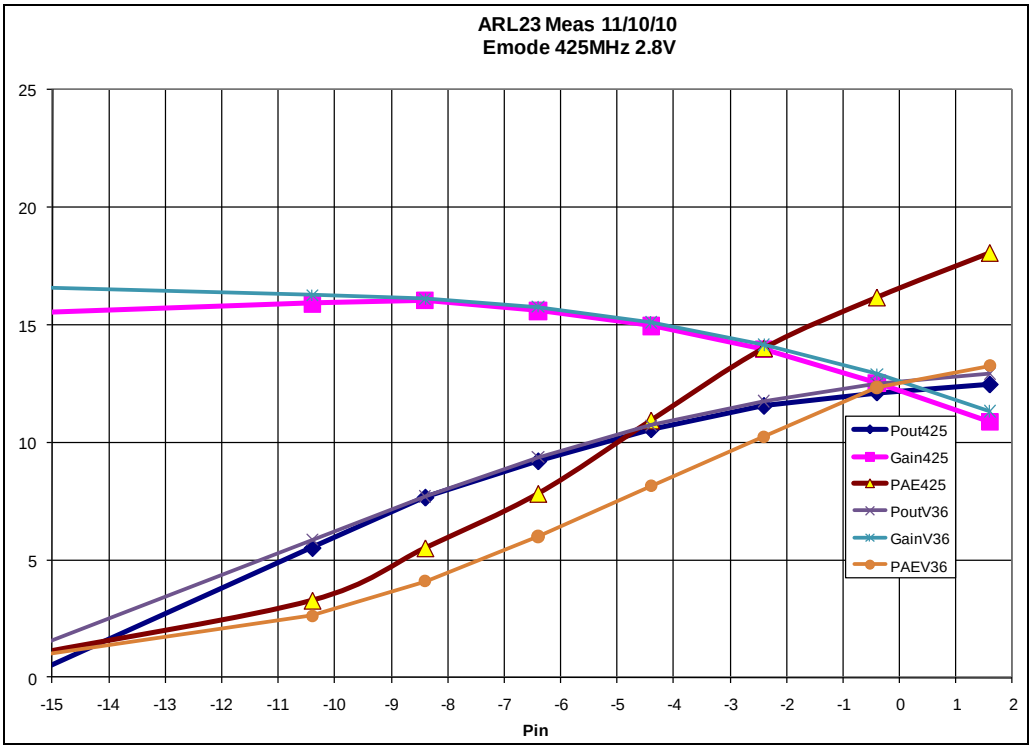

Figure 39. Plot of measured power performance of ARL23M425 at 2.8/3.6 V and 425 MHz.

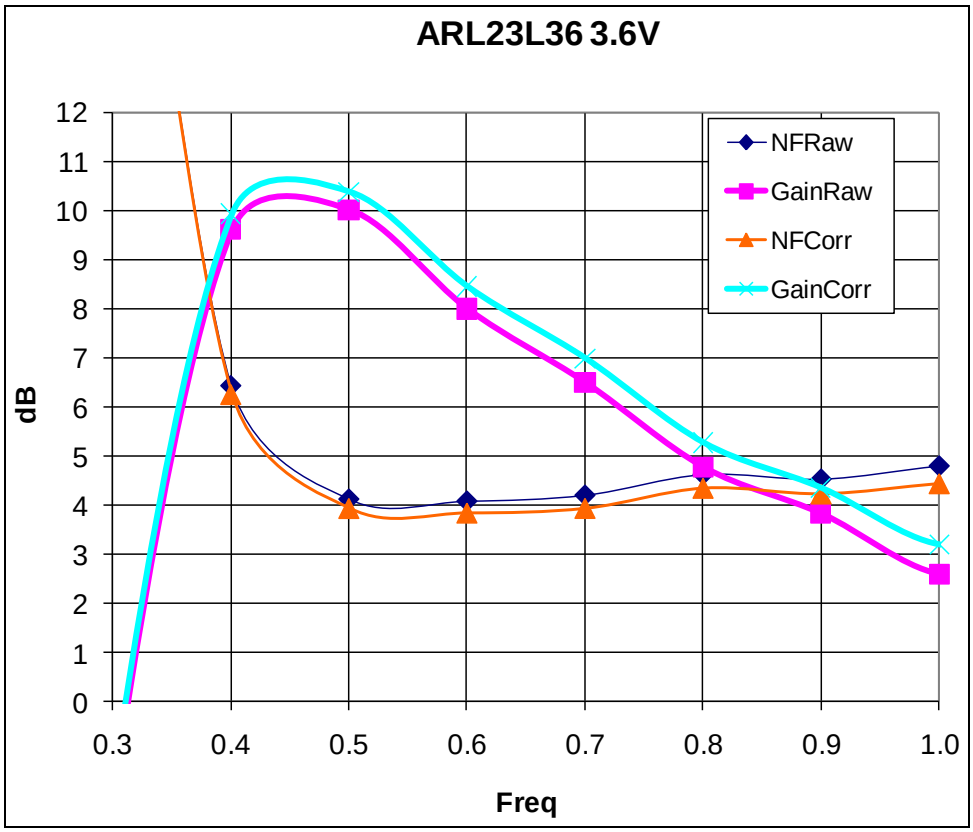

Figure 40. Plot of noise figure (yellow) and gain (cyan) of ARL23M425 at 3.6 V.

ARL24DB is a dual band front end RF IC containing a broadband BPSK modulator, a broadband power amplifier based on the 1st pass designs, a broadband low noise amplifier based on the 1st pass designs, and the TR switch. Tables 14 and 15 show the performance of the transmit path including the modulator, power amplifier, and TR switch at 425 MHz with 2.8 V and 3.6 V power supplies, respectively. Figure 41 plots the output power, gain, and PAE of the transmit path at 425 MHz with 2.8 V and 3.6 V supplies versus input power. Tables 16 and 17 show the performance of the transmit path including the modulator, power amplifier, and TR switch at 915 MHz with 2.8 V and 3.6 V power supplies, respectively. Figure 42 plots the output power, gain, and PAE of the transmit path at 915 MHz with 2.8 V and 3.6 V supplies versus input power. Performance at 915 MHz is similar to 425 MHz with lower gain. Figure 43 shows the measured performance of the receive path, which includes a broadband low noise amplifier and the TR switch at 3.6 V, where the "raw" lines show gain and noise figure including setup cable losses, and the "corr" lines show the true gain and noise figure. Past probe tests of the noise figure of the RF front end IC show a higher than expected noise figure, which might be due to allowing some of the TR switch control inputs to "float" to 0 V due to the limited number of DC needle probes available. Also included on ARL24DB was a probe testable copy of the broadband LNA where its individual performance is shown in figure 44. The noise figure of the individual LNA is about 2.5 dB, which corresponds to simulations. Current consumption for the

broadband LNA is 8 to 9 mA at 2.8 to 3.6 V, which is less than its 1st pass predecessor but still more than the narrowband LNA design. Gain (cyan line in figure 44) was approximately 15 dB at 425 MHz and 14 dB at 915 MHz for the individual LNA test circuit, and slightly less for the receive path of ARL24DB, which includes the additional insertion loss of the TR switch.

Table 14. Measured power performance of ARL24DB at 2.8 V and 425 MHz.

	11/12/2010								
425 MHz	Die#1	**ARL24DB ARLTILE2 TQPED**				2.8V ; 40 mA			
Pin(SG)	**Pout(SA)**	**Pin(corr)**	**Pout(corr)**	**Gain**	**I1(2.8V)**	**PDC(mw)**	**Pout(mw)**	**Drn Eff**	**PAE**
-15.0	1.17	-15.40	1.57	16.97	40	112.0	1.44	1.3	1.3
-10.0	6.17	-10.40	6.57	16.97	40	112.0	4.54	4.1	4.0
-8.0	8.17	-8.40	8.57	16.97	39	109.2	7.19	6.6	6.5
-6.0	9.83	-6.40	10.23	16.63	39	109.2	10.54	9.7	9.4
-4.0	11.33	-4.40	11.73	16.13	37	103.6	14.89	14.4	14.0
-2.0	12.33	-2.40	12.73	15.13	35	98.0	18.75	19.1	18.5
0.0	12.83	-0.40	13.23	13.63	34	95.2	21.04	22.1	21.1

Table 15. Measured power performance of ARL24DB at 3.6 V and 425 MHz.

425 MHz	Die#1	**ARL24DB ARLTILE2 TQPED**				3.6V ; 42 mA			
Pin(SG)	**Pout(SA)**	**Pin(corr)**	**Pout(corr)**	**Gain**	**I1(3.6V)**	**PDC(mw)**	**Pout(mw)**	**Drn Eff**	**PAE**
-15.0	1.17	-15.40	1.57	16.97	42	151.2	1.44	0.9	0.9
-10.0	6.17	-10.40	6.57	16.97	42	151.2	4.54	3.0	2.9
-8.0	8.17	-8.40	8.57	16.97	42	151.2	7.19	4.8	4.7
-6.0	9.83	-6.40	10.23	16.63	42	151.2	10.54	7.0	6.8
-4.0	11.33	-4.40	11.73	16.13	41	147.6	14.89	10.1	9.8
-2.0	12.50	-2.40	12.90	15.30	41	147.6	19.50	13.2	12.8
0.0	13.33	-0.40	13.73	14.13	40	144.0	23.60	16.4	15.8
2.0	13.67	1.60	14.07	12.47	39	140.4	25.53	18.2	17.2

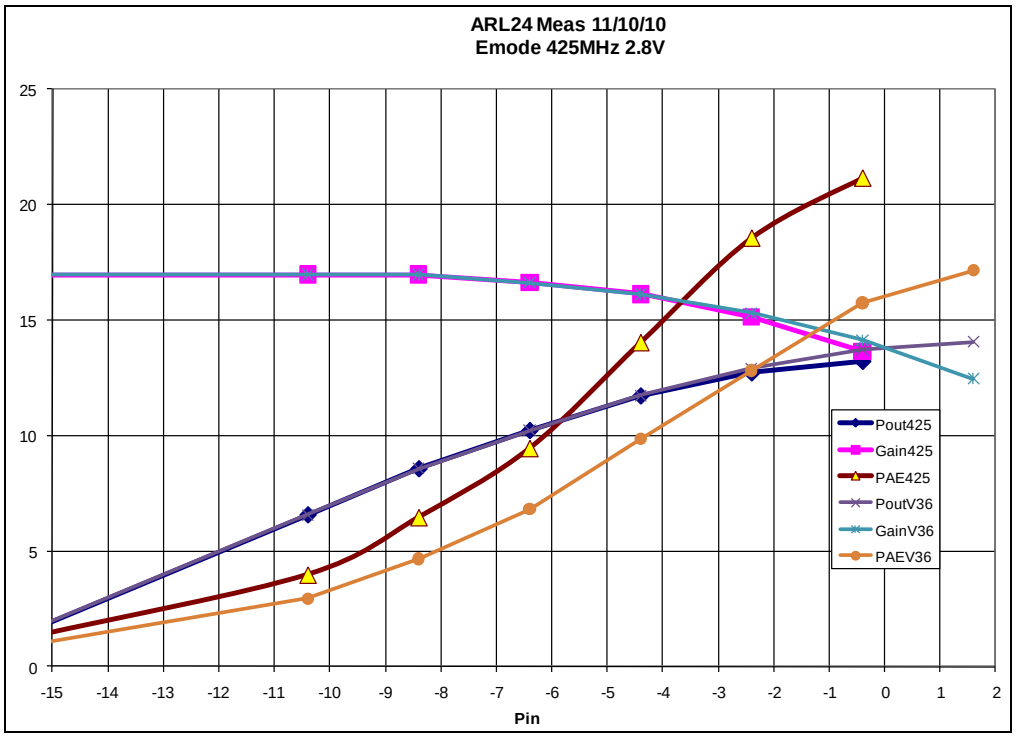

Figure 41. Plot of measured power performance of ARL24DB at 2.8/3.6 V and 425 MHz.

Table 16. Measured power performance of ARL24DB at 2.8 V and 915 MHz.

	11/12/2010								
915 MHz	Die#1	**ARL24DB ARLTILE2 TQPED**				2.8V ; 40 mA			
Pin(SG)	**Pout(SA)**	**Pin(corr)**	**Pout(corr)**	**Gain**	**I1(2.8V)**	**PDC(mw)**	**Pout(mw)**	**Drn Eff**	**PAE**
-15.0	-3.33	-15.55	-2.78	12.77	40	112.0	0.53	0.5	0.4
-10.0	1.33	-10.55	1.88	12.43	40	112.0	1.54	1.4	1.3
-8.0	3.33	-8.55	3.88	12.43	40	112.0	2.44	2.2	2.1
-6.0	5.33	-6.55	5.88	12.43	40	112.0	3.87	3.5	3.3
-4.0	7.33	-4.55	7.88	12.43	40	112.0	6.14	5.5	5.2
-2.0	9.33	-2.55	9.88	12.43	39	109.2	9.73	8.9	8.4
0.0	11.17	-0.55	11.72	12.27	38	106.4	14.86	14.0	13.1
2.0	12.33	1.45	12.88	11.43	36	100.8	19.41	19.3	17.9
4.0	13.17	3.5	13.72	10.3	34	95.2	23.55	24.7	22.4

Table 17. Measured power performance of ARL24DB at 3.6 V and 915 MHz.

915 MHz	Die#1	**ARL24DB ARLTILE2 TQPED**				3.6V ; 43 mA			
Pin(SG)	**Pout(SA)**	**Pin(corr)**	**Pout(corr)**	**Gain**	**I1(3.6V)**	**PDC(mw)**	**Pout(mw)**	**Drn Eff**	**PAE**
-15.0	-3.83	-15.55	-3.28	12.27	43	154.8	0.47	0.3	0.3
-10.0	1.33	-10.55	1.88	12.43	42	151.2	1.54	1.0	1.0
-8.0	3.33	-8.55	3.88	12.43	42	151.2	2.44	1.6	1.5
-6.0	5.33	-6.55	5.88	12.43	42	151.2	3.87	2.6	2.4
-4.0	7.33	-4.55	7.88	12.43	42	151.2	6.14	4.1	3.8
-2.0	9.33	-2.55	9.88	12.43	42	151.2	9.73	6.4	6.1
0.0	11.17	-0.55	11.72	12.27	41	147.6	14.86	10.1	9.5
2.0	12.50	1.45	13.05	11.60	41	147.6	20.18	13.7	12.7
4.0	13.50	3.45	14.05	10.6	40	144.0	25.41	17.6	16.1

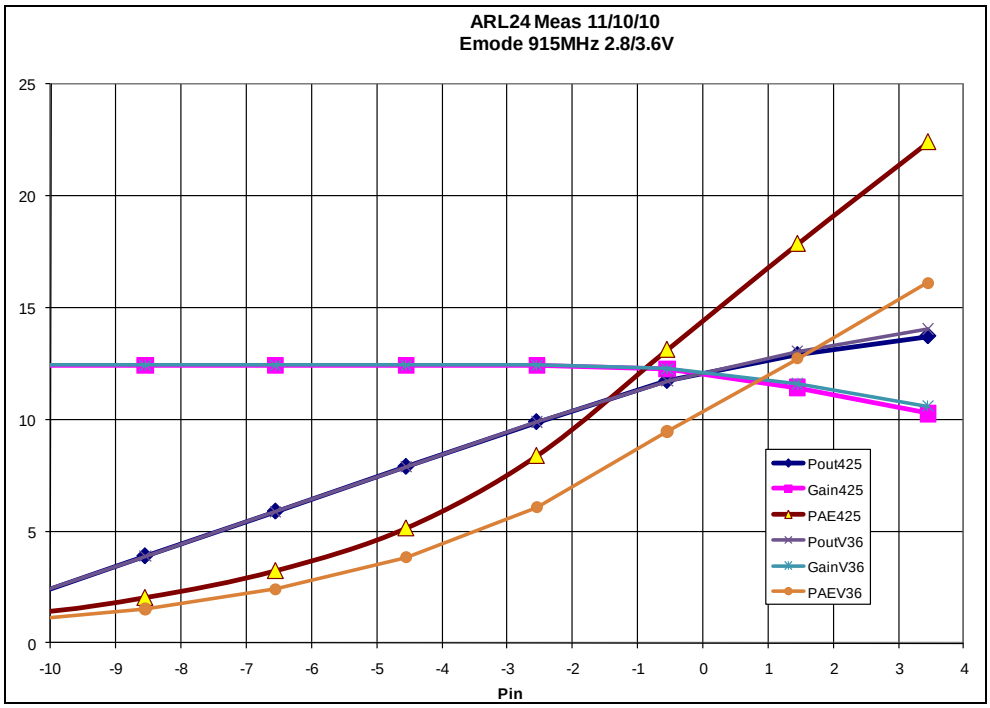

Figure 42. Plot of measured power performance of ARL24DB at 2.8/3.6 V and 915 MHz.

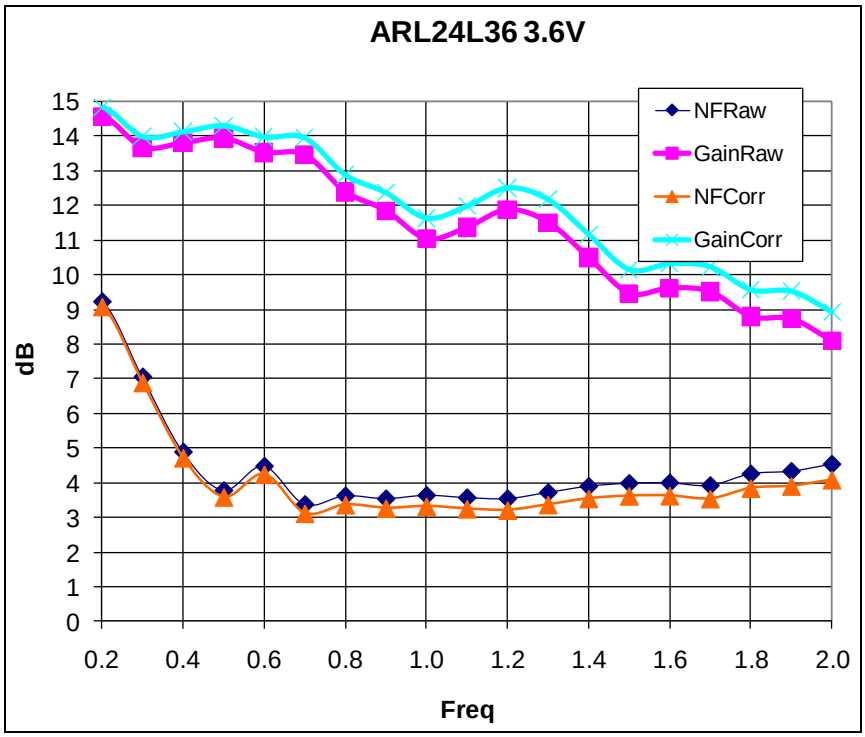

Figure 43. Plot of noise figure (yellow) and gain (cyan) of ARL24DB at 3.6 V.

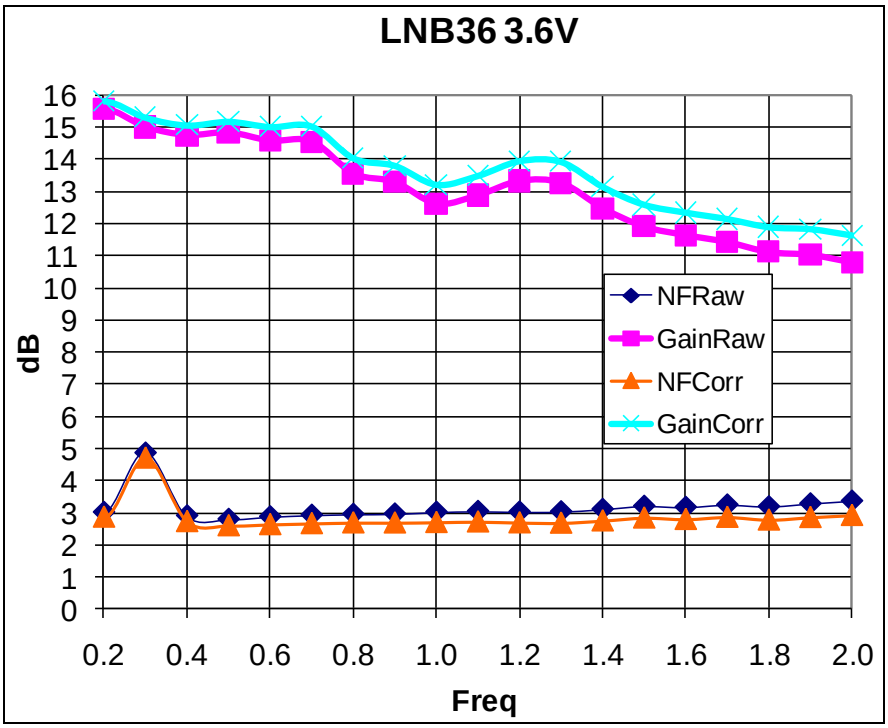

Figure 44. Plot of noise figure (yellow) and gain (cyan) of broadband LNA at 3.6 V (ARL24DB).

4. Die Testing of Passive (Matching) 2nd Pass Designs

Following is a summary of the passive design tests using a probe station for bare die testing. Two designs are mostly passive but include PHEMT switches, which draw negligible current. Both switched designs are intended to select one of two possible RF connections. The single antenna connection can be switched to either a separate input for the transmit path, or a separate output for the receive path to be compatible with the booster IC designs. The second switched design also allows a selection of either a 425 MHz band matching circuit or a 915 MHz band matching circuit, presumably to be used in combination with the dual band active booster IC (ARL24DB). Matching circuits for the Texas Instruments (TI) CC1000 sub-1 GHz transceiver and the more recent TI CC1100 sub-1 GHz transceiver were designed for targeting a combined COTS RFIC and ARL booster IC. There seemed to be some discrepancies in the data sheets for the two TI RFICs, so a best guess of the desired match was used for the designs. Parasitic effects of the switches were expected to be small and were ignored for the matching circuit design. For the passive circuits, measurements are compared to simulations of the designs with good agreement.

- ARL26DB—This dual band design contains a matching circuit plus RF switches to connect the integrated matching circuit for a TI CC1100 RFIC for operation at either 425 or 900 MHz. One side of the design connects to the differential RF connections of the

CC1100 RFIC and the other side switches to one of two single ended RF connections, intended to be either an input to a transmitter/power amplifier or an output from a receiver/low noise amplifier.

ARL26DB is a dual-band matching circuit intended to work with the CC1100 series RFIC from TI. The schematic shown in figure 45 consists of the recommended matching circuit for 433 MHz (top middle) and the recommended matching circuit for 915 MHz (bottom middle), which can be switched to the differential RF ports of a CC1100 (1 and 2 on left) so that one band or the other is selected at any given time. Additional switches choose between one of two antenna connections (A1 and A2), which are intended to be the separate single-ended RF connections of the transmit and receive paths of the 2nd pass booster IC designs. Figures 46, 47, and 48 show good agreement between s-parameter measurements (solid) and simulations (dotted) for the three RF connections when the antenna port is switched to 433 MHz operation. Likewise, figures 49, 50, and 51 show good agreement between s-parameter measurements (solid) and simulations (dotted) for the three RF connections when the antenna port is switched to 915 MHz operation. While the matching circuit should be tested in a board level design with the intended CC1100 design, it should be noted that the s-parameters are relatively close to the 50-ohm match point of the center of the Smith Chart. It would seem that the newer CC1100 design was intended to have a lower Q match near 50 ohms, while the older CC1000 matches often seem to be closer to the edge of the Smith Chart, indicating a circuit that might be difficult to match to 50 ohms. The preference would be to use the newer CC1100 design with the appropriate matching circuit designs, though there may be existing CC1000 applications that could benefit from the improved SWAP provided by the integrated matching circuits intended for the CC1000 RFIC.

- ARL27M425—This design contains discrete lumped elements circuits for an integrated match at 425-MHz circuit for a TI CC1000 RFIC. It separates the recommended matching circuit into an RF input and RF output match for separate connections as either an input to a transmitter/power amplifier or an output from a receiver/low noise amplifier, rather than a single-ended connection to an antenna.

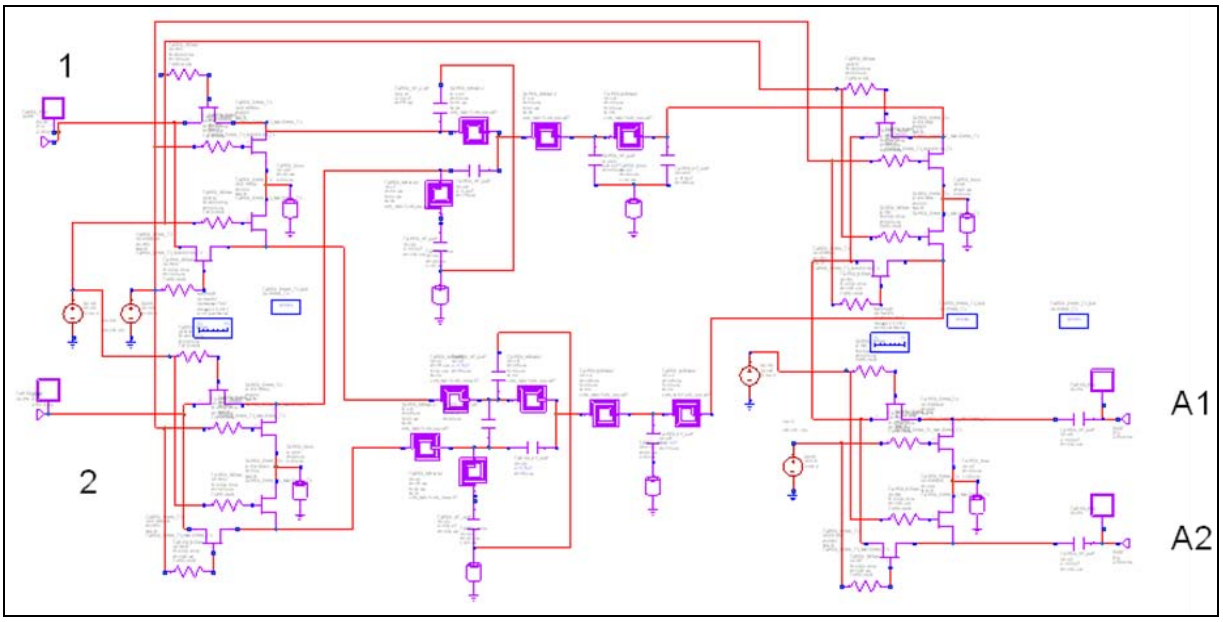

Figure 45. Schematic of ARL26DB 425/915 MHz dual band matching circuit for the CC1100.

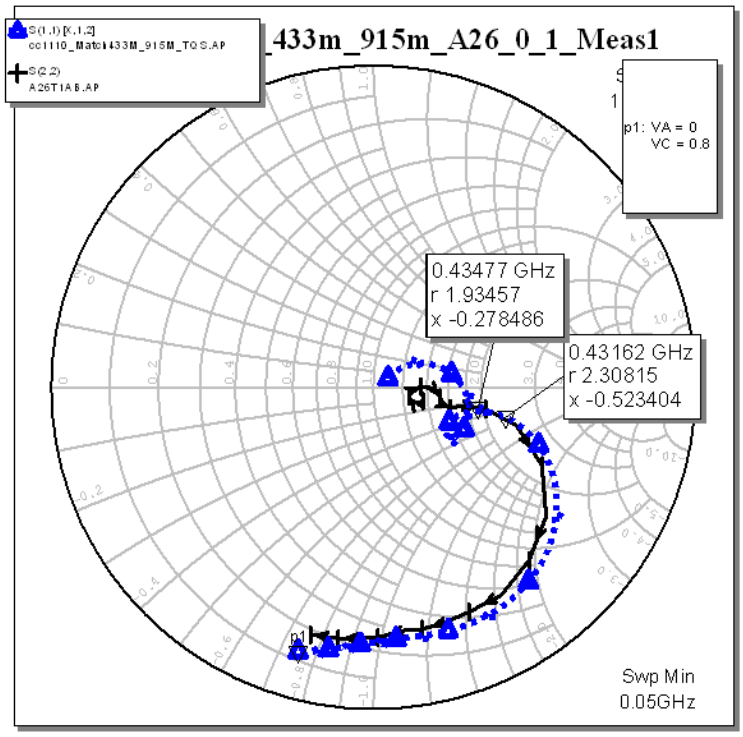

Figure 46. Measured (solid) versus simulation (dotted) of S11 for ARL26DB (433 MHz match).

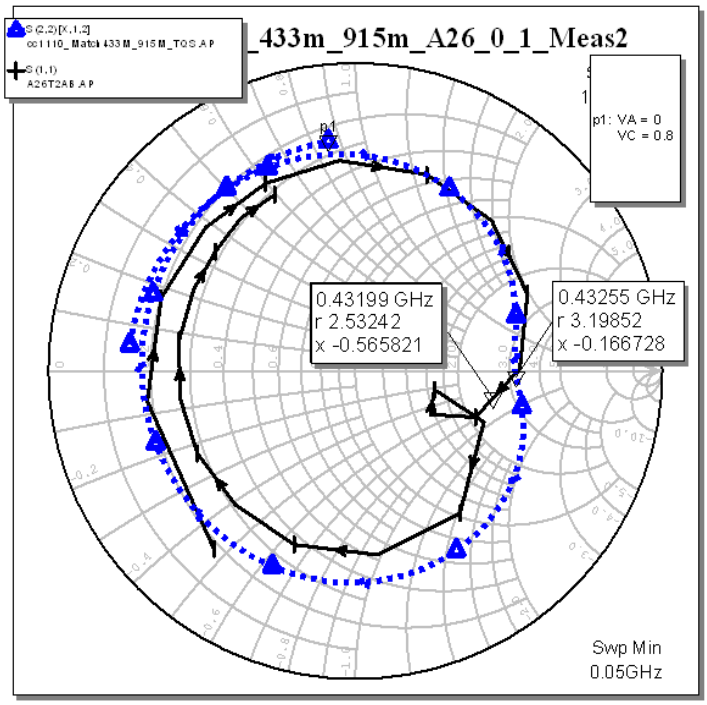

Figure 47. Measured (solid) versus simulation (dotted) of S22 for ARL26DB (433 MHz match).

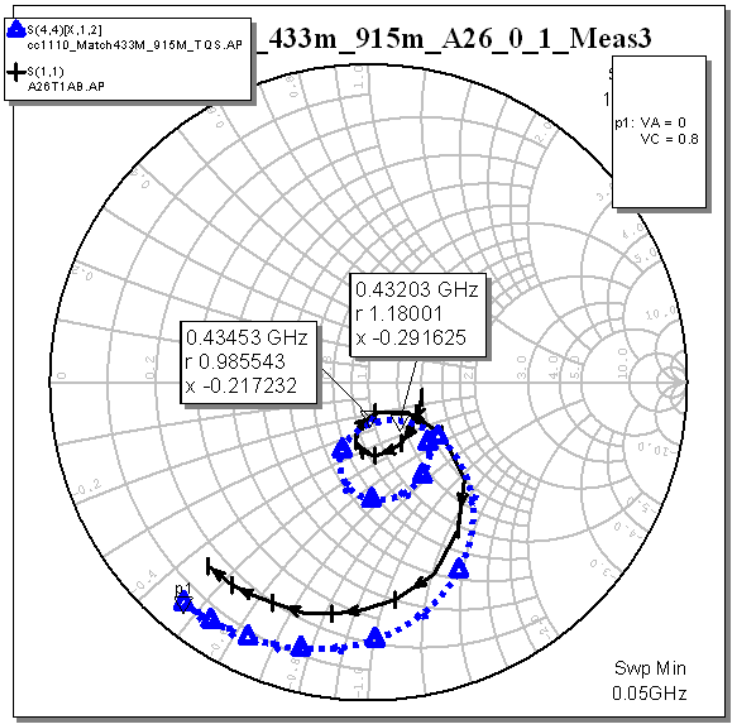

Figure 48. Measured (solid) versus simulation (dotted) of antenna connection for ARL26DB (433 MHz match).

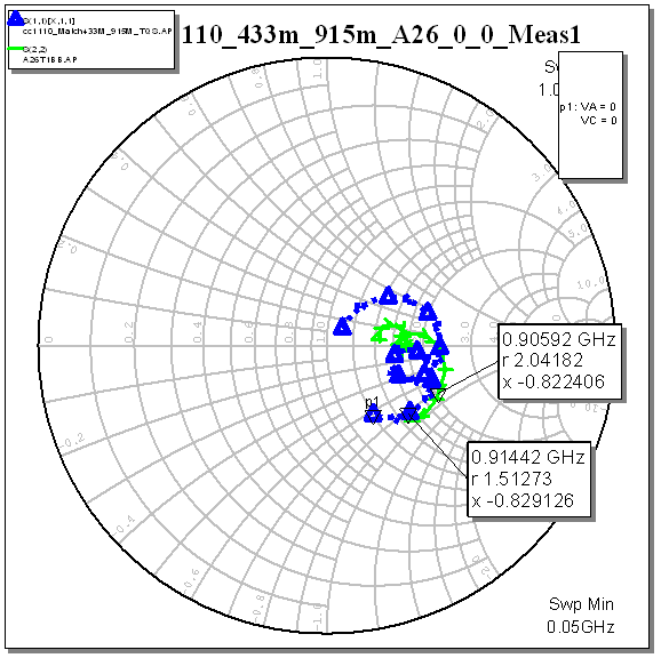

Figure 49. Measured (solid) versus simulation (dotted) of S11 for ARL26DB (915 MHz match).

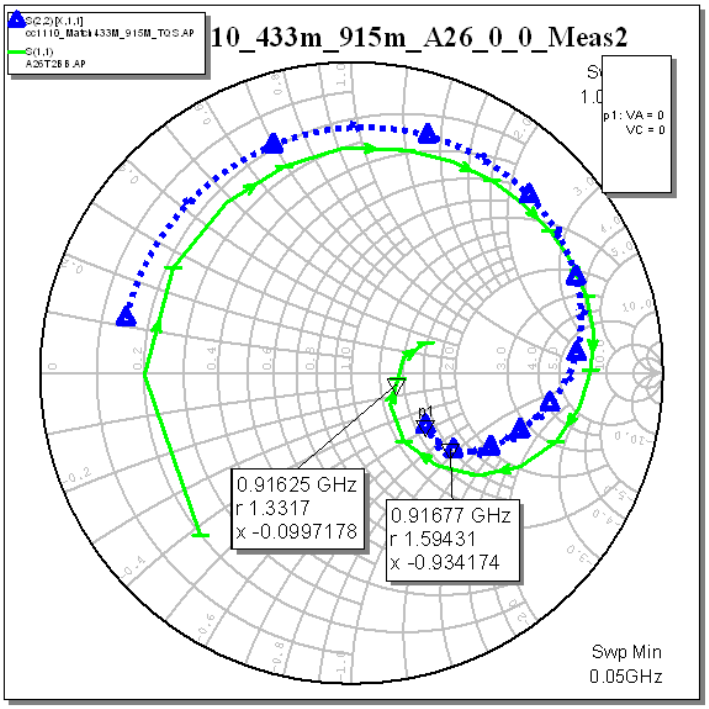

Figure 50. Measured (solid) versus simulation (dotted) of S22 for ARL26DB (915 MHz match).

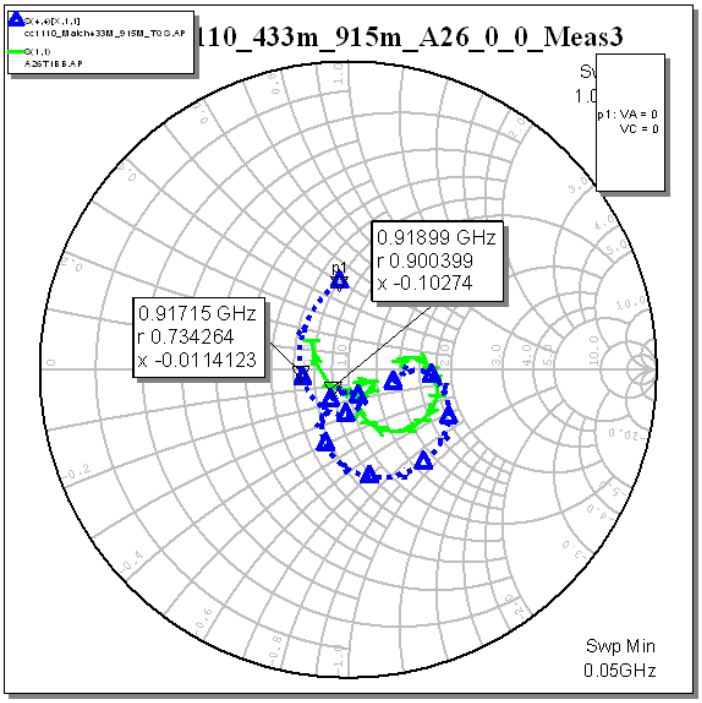

Figure 51. Measured (solid) versus simulation (dotted) of antenna connection for ARL26DB (915 MHz match).

ARL27M425 is a matching circuit intended to work with the CC1000 series RFIC from TI. The schematic shown in figure 52 splits the match for the transmit (4 PA) and receive path (2 LNA) of the booster IC into a simple shunt inductor/series capacitor match, followed by an identical three-element, low-pass filter. Figure 53 shows reasonable agreement between s-parameter measurements (solid) and simulations (dotted) for the receive path booster IC RF connections to the CC1000 RF input at 433 MHz. Note that the CC1000 looks more difficult to match, as its s-parameters are not as well-behaved as the CC1100 designs in a 50-ohm system. Likewise, figure 54 shows reasonable agreement between s-parameter measurements (solid) and simulations (dotted) for the transmit path booster IC RF connection to the CC1000 RF output at 433 MHz.

- ARL28M900—This design contains discrete lumped elements circuits for an integrated match at 900-MHz circuit for a TI CC1000 RFIC. It separates the recommended matching circuit into an RF input and RF output match for separate connections as either an input to a transmitter/power amplifier or an output from a receiver/low noise amplifier, rather than a single-ended connection to an antenna. It is similar to ARL27M425, except for the frequency of operation.

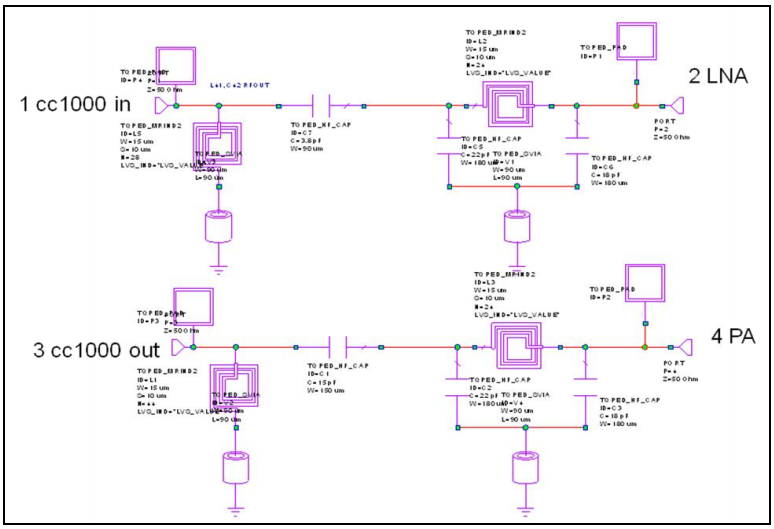

Figure 52. Schematic of ARL27M425 425 MHz band matching circuit for the CC1000.

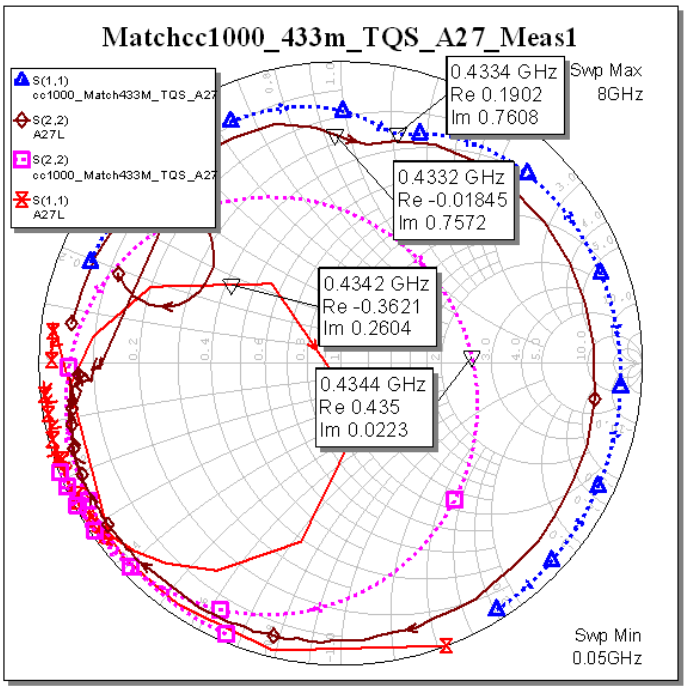

Figure 53. Measured (solid) versus simulation (dotted) of receive path for CC1000 (425 MHz match).

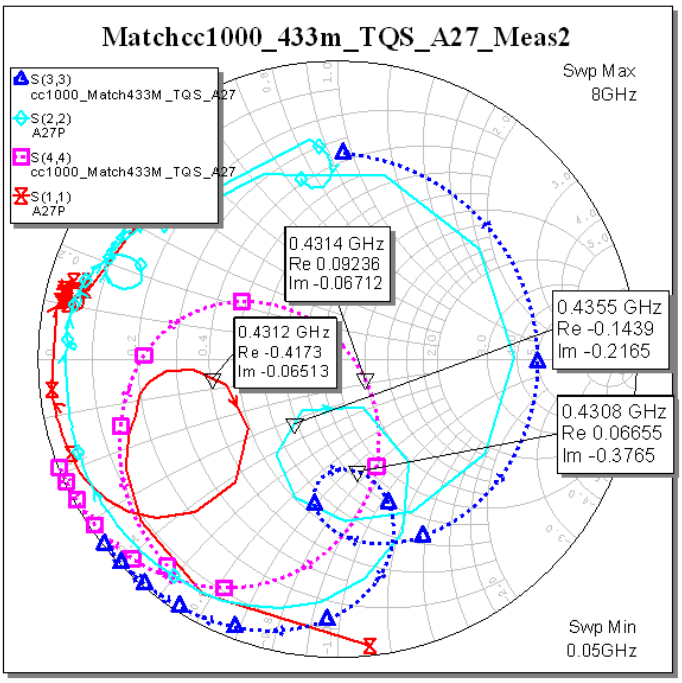

Figure 54. Measured (solid) versus simulation (dotted) of transmit path for CC1000 (425 MHz match).

ARL28M900 is a matching circuit intended to work with the CC1000 series RFIC from TI. The schematic is the same as the previous design (figure 52), which splits the match for the transmit (4 PA) and receive path (2 LNA) of the booster IC into a simple shunt inductor/series capacitor match, followed by an identical three-element low-pass filter. The matching element values are different than the 433 MHz design, but the topology is the same. Figure 55 shows reasonable agreement between s-parameter measurements (solid) and simulations (dotted) for the receive path booster IC RF connection to the CC1000 RF input at 915 MHz. Note that the CC1000 looks more difficult to match, as its s-parameters are not as well-behaved as the CC1100 designs in a 50-ohm system. Likewise, figure 56 shows reasonable agreement between s-parameter measurements (solid) and simulations (dotted) for the transmit path booster IC RF connection to the CC1000 RF output at 915 MHz.

- ARL29M425—This single band design contains a matching circuit to connect the integrated matching circuit for a TI CC1100 RFIC for operation at 425 MHz. One side of the design connects to the differential RF connections of the CC1100 RFIC, and the other side connects to a single-ended RF connection, intended to be the antenna connection.

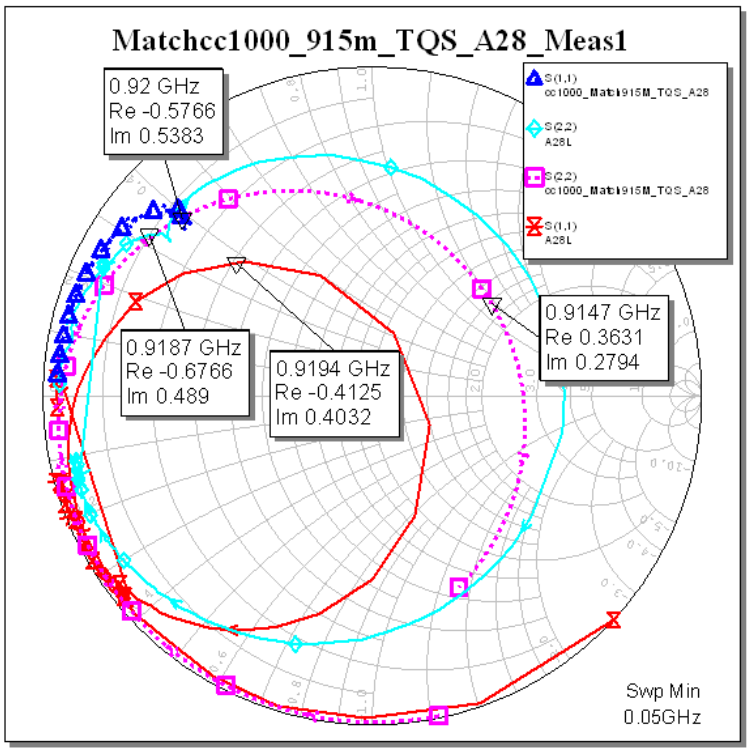

Figure 55. Measured (solid) versus simulation (dotted) of receive path for CC1000 (915 MHz match).

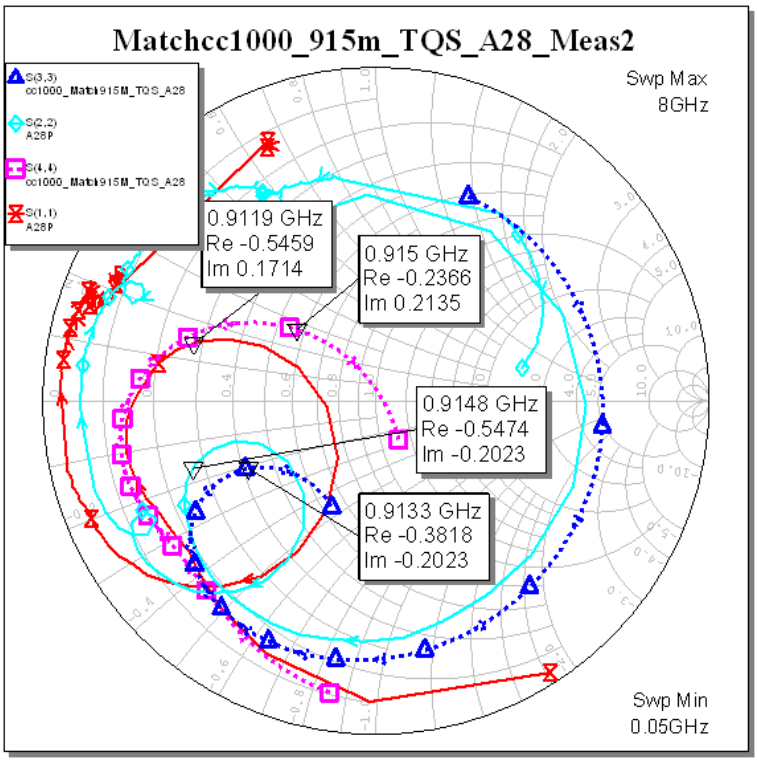

Figure 56. Measured (solid) versus simulation (dotted) of transmit path for CC1000 (915 MHz match).

ARL29M425 is a matching circuit intended to work with the CC1100 series RFIC from TI. It could improve SWAP in existing designs using discrete matching elements for the CC1000. The schematic shown in figure 57 consists of the recommended matching circuit for 433 MHz and was used for the 433 MHz matching circuit portion of the ARL26DB dual band design. This IC would replace the discrete matching elements required to connect the CC1100 to a single-ended 50-ohm antenna connection. An external RF switch would be needed for operation with the 2nd pass booster IC designs. The next design, ARL29M425S, is exactly the same matching circuit but includes the RF switch to connect to either the transmit or the receive RF connections of the booster IC. Figures 58, 59, and 60 show good agreement between s-parameter measurements (solid) and simulations (dotted) of the three RF connections for the 433 MHz band. As stated before with the similar ARL26DB design, it should be noted that the s-parameters are relatively close to the 50-ohm match point of the center of the Smith Chart.

- ARL29M425S—This single band design contains a matching circuit to connect the integrated matching circuit for a TI CC1100 RFIC for operation at 425 MHz. One side of the design connects to the differential RF connections of the CC1100 RFIC, and the other side connects to RF switches intended for connection to the input of a transmitter/power amplifier or an output from a receiver/low noise amplifier, rather than the single-ended connection to an antenna. ARL29M425 is a similar design.

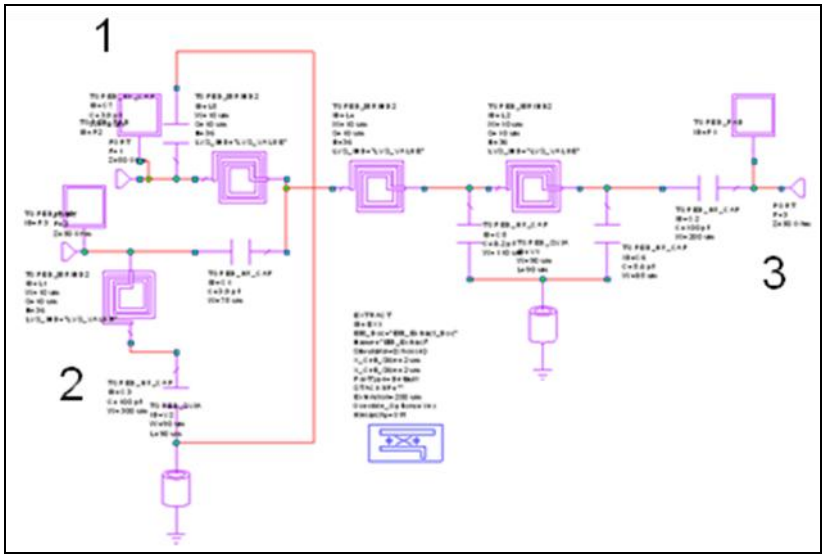

Figure 57. Schematic of ARL29M425 425 MHz band matching circuit for the CC1100.

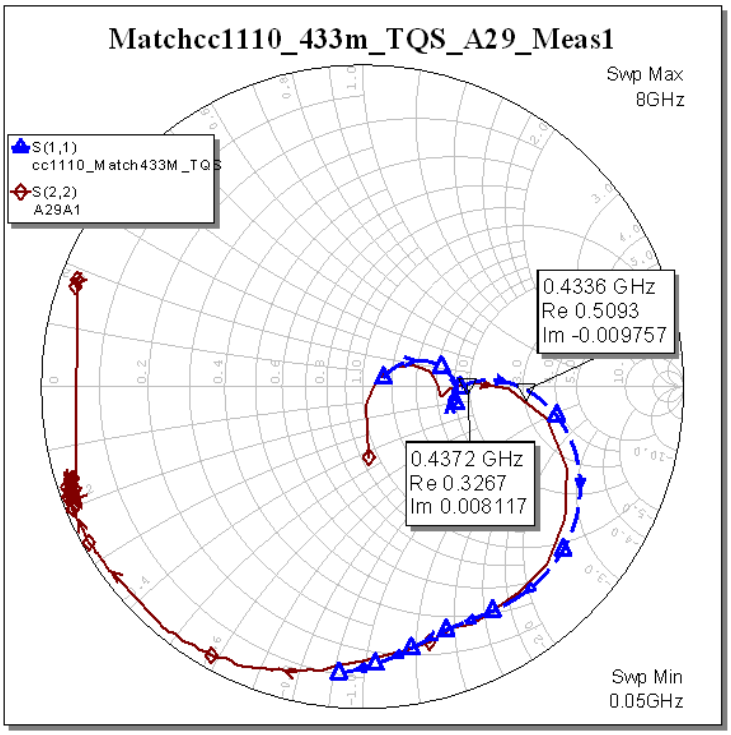

Figure 58. Measured (solid) versus simulation (dotted) of S11 for ARL29M425 (425 MHz match).

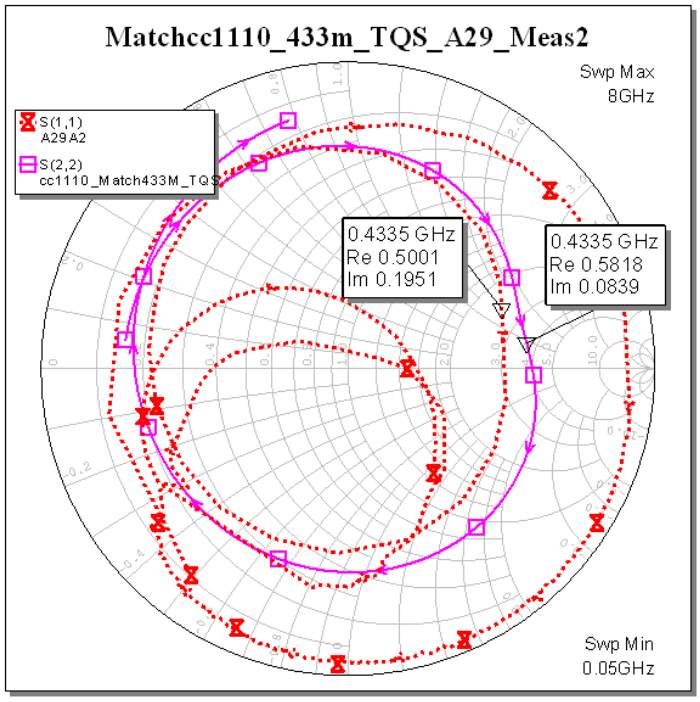

Figure 59. Measured (solid) versus simulation (dotted) of S22 for ARL29M425 (425 MHz match).

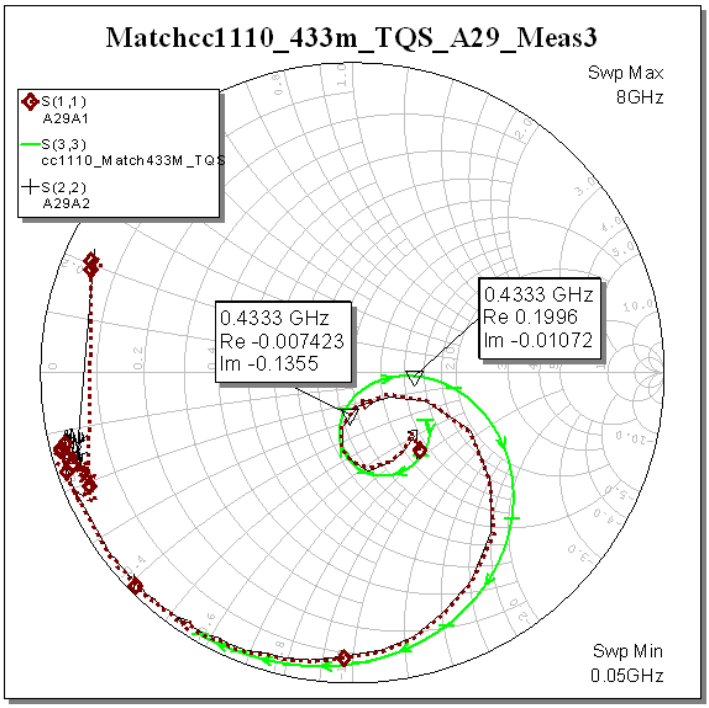

Figure 60. Measured (solid) versus simulation (dotted) of antenna connection for ARL29M425 (425 MHz match).

ARL29M425S is a matching circuit intended to work with the CC1100 series RFIC from TI, identical to the previous design but with the addition of PHEMT switches to connect to either one of two RF antenna connections. Figures 61, 62, and 63 show good agreement between s-parameter measurements (solid) and simulations (dotted) for the three RF connections for the 433 MHz band. The results are very similar to the non-switched version of the integrated matching circuit, ARL29M425.

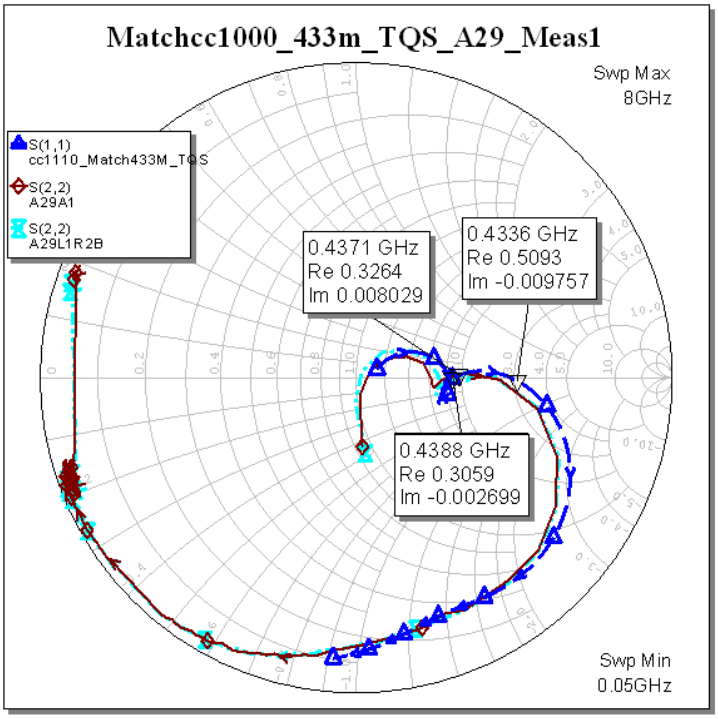

Figure 61. Measured (solid) versus simulation (dotted) of S11 for ARL29M425S (425 MHz match).

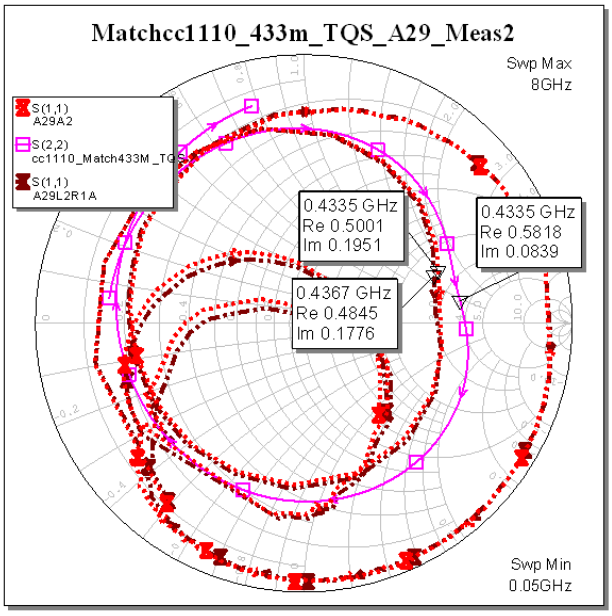

Figure 62. Measured (solid) versus simulation (dotted) of S22 for ARL29M425S (425 MHz match).

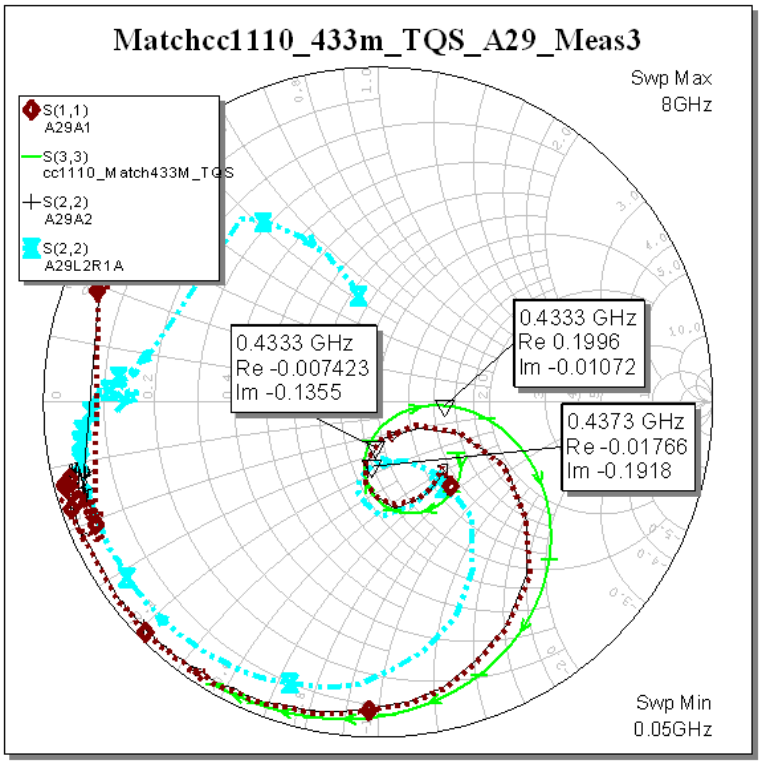

Figure 63. Measured (solid) versus simulation (dotted) of S33 for ARL29M425S (425 MHz match).

5. Conclusion

All of the designs worked successfully in the die testing. Figure 64 shows the 10 designs fabricated with TriQuint's 0.5 µm TQPED PHEMT process. The active designs are the bottom four and the right middle large die (ARL21 to 25). Integrated Matching circuit designs are the large left middle die and the top four smaller die sites (ARL26 to 29/29S).

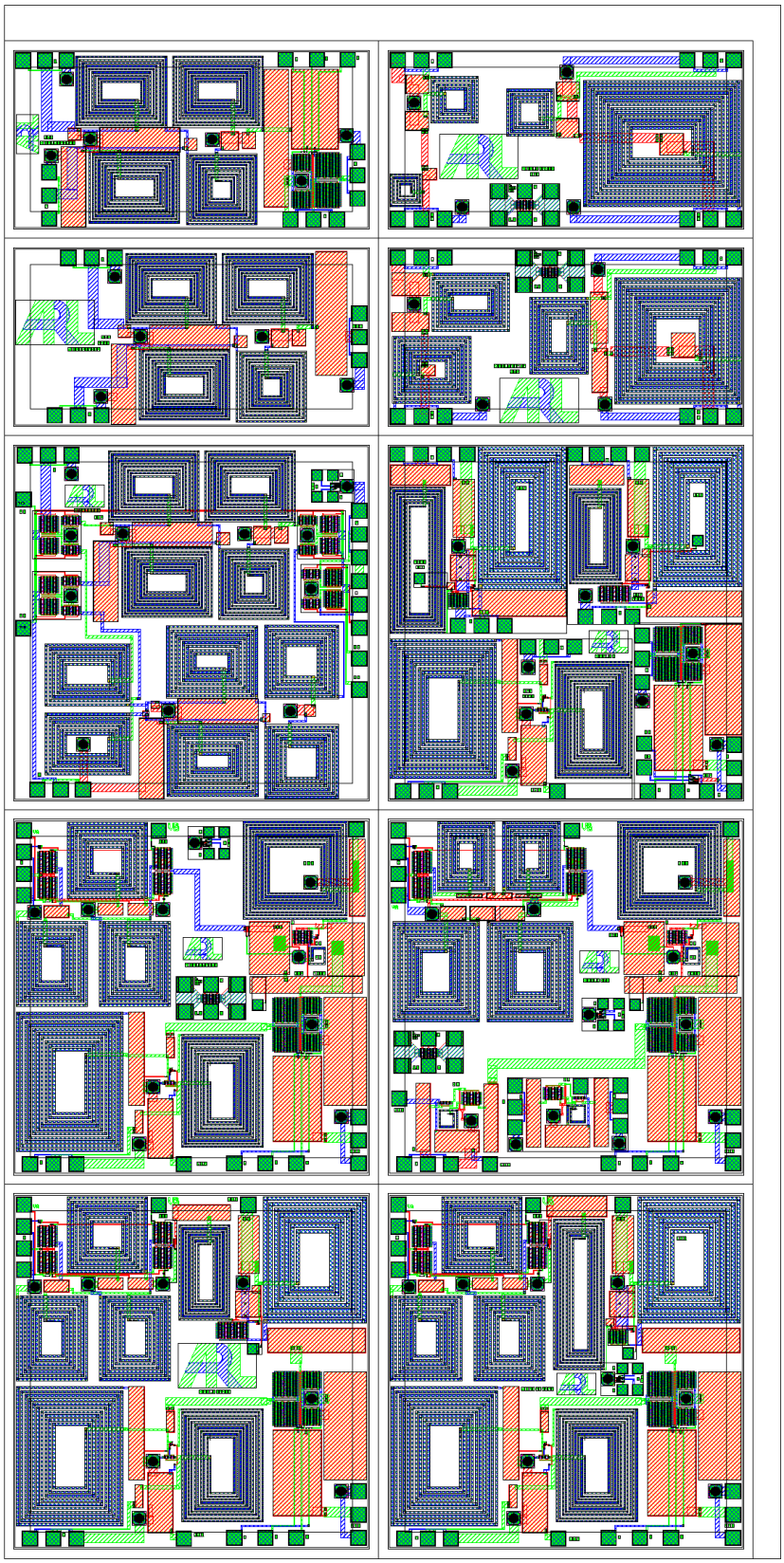

Figure 64. 5 mm x 10 mm GaAs quarter tile of the ten 2nd pass booster IC designs.

Power performance of the amplifiers was less than desired, but additional tests of the designs will be performed in packaged ICs on PC boards with RF connectors. Noise figure performance is expected to improve for the receive paths of the RF front end designs that were probed with one or more floating DC inputs, due to probe test limitations. When the package tests are complete, analysis should be performed to see if the power efficiencies can be optimized further in future designs. For the passive designs that integrate matching circuits for the TI CC1000 and CC1100 RFICs, system level boards will need to be created and tested. Certainly, the passive designs already show the improved SWAP compared to the many discrete matching elements that are required for board level integration of COTS RFICs. These matching designs may need to be "tweaked" or optimized at the system level. The current matching circuit documentation for the targeted CC1000 and CC1100 devices seemed to be deficient in some areas. Future tests should help clarify how well these current designs work at the system level. For further documentation of the previous 1st pass designs and the current 2nd pass designs, see the references 1–6.

Standard size 6×50 µm probeable Dmode and Emode PHEMTs were part of the tile fabrication and were measured but not included with the test data. The measured results up to 2 GHz compared well with the device models. In future fabrications, it would be good to add devices of the same size as the circuit designs, as it would be easier to re-simulate the designs using measured device data from the same wafer fabrication. For instance, the 50 mW amplifier used a 6×80 µm Emode PHEMT and the 100 mW used a 10×96 µm Emode PHEMT. A model could be extracted from the measured 6×50 µm Emode test device and then scaled to these two device sizes, but the calibration for these device tests did not appear to be as good as desired.

6. References

1. Mitchell, G.; Penn, J. *Preliminary Gallium Arsenide (GaAs) Integrated Circuit Design for Radio Frequency Booster Chips at 450, 900, and 2400 MHz*; ARL-TR-4970; U.S. Army Research Laboratory: Adelphi, MD, September 2009.

2. Penn, J. GaAs *Microwave Integrated Circuit Designs Submitted to TriQuint Semiconductor for Fabrication*; ARL-TN-0381; U.S. Army Research Laboratory: Adelphi, MD, December 2009.

3. Mitchell, G.; Penn, J. *Results of Bare Die Probing for RF Booster Chip at 400, 900, and 2400 MHz*; ARL-TR-5170, U.S. Army Research Laboratory: Adelphi, MD, April 2010.

4. Penn, J. *Testing of GaAs Microwave Integrated Circuit Designs in QFN Packages*; ARL-TR-5131, U.S. Army Research Laboratory: Adelphi, MD, March 2010

5. Penn, J. *GaAs Microwave Integrated Circuit Designs Submitted to TriQuint Semiconductor for Fabrication (ARL Tile #2)*; ARL-TN-0404; U.S. Army Research Laboratory: Adelphi, MD, September 2010.

6. Penn, J. *Optimized (2nd Pass) Gallium Arsenide (GaAs) Integrated Circuit Radio Frequency (RF) Booster Designs for 425 MHz and Dual Band (425 and 900 MHz)*; ARL-TR-5396; U.S. Army Research Laboratory: Adelphi, MD, October 2010.

List of Symbols, Abbreviations, and Acronyms

ADS	Advanced Design System
BPSK	Binary Phase Shift Key
GaAs	gallium arsenide
IC	Integrated Circuit
LNA	Low Noise Amplifier
MWO	Microwave Office
PAE	power added efficiency
PHEMT	Pseudomorphic High Electron Mobility Transistor
RF	Radio Frequency
RFIC	Radio Frequency Integrated Circuit
SWAP	size, weight, and power
TI	Texas Instruments
TR	transmit/receive

NO. OF COPIES ORGANIZATION

1 (PDF only) DEFENSE TECHNICAL INFORMATION CTR
DTIC OCA
8725 JOHN J KINGMAN RD
STE 0944
FORT BELVOIR VA 22060-6218

1 DIRECTOR
US ARMY RESEARCH LAB
IMNE ALC HRR
2800 POWDER MILL RD
ADELPHI MD 20783-1197

1 DIRECTOR
US ARMY RESEARCH LAB
RDRL CIM L
2800 POWDER MILL RD
ADELPHI MD 20783-1197

1 DIRECTOR
US ARMY RESEARCH LAB
RDRL CIM P
2800 POWDER MILL RD
ADELPHI MD 20783-1197

11 DIRECTOR
US ARMY RESEARCH LAB
RDRL SER
PAUL AMIRTHARAJ
RDRL SER E
ROMEO DEL ROSARIO
GREG MITCHELL
JAMES WILSON
GLEN BIRDWELL
ROB REAMS
JOHN PENN (3 HCS)
ED VIVEIROS
RDRL SEG
STEVE RAGER
2800 POWDER MILL RD
ADELPHI MD 20783-1197

1 CERDEC I2WD
RDER IWR CI
BOB GROSS
SUITE D
6240 GUARDIAN GATEWAY
APG MD 21005

1 I2WD
STEVE HAUGHT
FT MONMOUTH NJ

ABERDEEN PROVING GROUND

1 DIR USARL
RDRL CIM G (BLDG 4600)

INTENTIONALLY LEFT BLANK.